Equilibrium-Based NFT Marketplace Recommendation for NFTs with Breeding

Chin-Yuan Yeh[1,3], Hsi-Wen Chen[2,3], De-Nian Yang[3,4], Wang-Chien Lee[5], Philip S. Yu[6], Ming-Syan Chen[1,2]
[1] *Graduate Institute of Communication Engineering, National Taiwan University, Taiwan*
[2] *Department of Electrical Engineering, National Taiwan University, Taiwan*
[3] *Institute of Information Science, Academia Sinica, Taiwan*
[4] *Research Center for Information Technology Innovation, Academia Sinica, Taiwan*
[5] *Department of Computer Science and Engineering, The Pennsylvania State University, USA*
[6] *Department of Computer Science, University of Illinois Chicago, USA*
{cyyeh, hwchen}@arbor.ee.ntu.edu.tw, dnyang@iis.sinica.edu.tw
wlee@cse.psu.edu, psyu@uic.edu, mschen@ntu.edu.tw

***Abstract*—Recently, Non-Fungible Tokens (NFTs) have attracted attention as valuable digital assets. However, NFT marketplaces face complex challenges in simultaneously recommending optimal pricing to sellers and desirable NFTs to buyers. Unlike conventional marketplaces that focus only on balancing demand and supply between sellers and buyers, these tasks are complicated by intricate value interdependencies arising from diverse buyer preferences, budgets, *trait* rarities, and the unprecedented *breeding mechanisms*. This paper formulates the *NFT Project Pricing/Purchasing Recommendation (NP^{3}R)* problem, aiming to achieve a competitive equilibrium that concurrently optimizes seller revenue and buyer utility. We introduce *BANTER*, an iterative algorithm that jointly determines (1) optimal NFT purchases for buyers (via NFT-REC), considering breeding utility and current prices; and (2) optimal pricing for sellers (via PRICE-REC), based on aggregated demand from NFT-REC. To efficiently manage the combinatorial complexity of breeding, we devise *Optimal Parent Pair Selection (OPPS)* and *Heterogeneous Parent Set Selection (HPSS)* schemes. Theoretical analysis guarantees BANTER to converge to a competitive equilibrium. Experiments on five real-world NFT datasets demonstrate its effectiveness in enhancing both seller revenue and average buyer utility. Source code: https://github.com/jimmy-academia/BANTER**

I. INTRODUCTION

Non-fungible tokens (NFTs) have emerged as significant digital assets, representing unique digital art and collectibles.[1] By 2030, the total market value of NFTs is projected to grow up to \$80B. Beyond individual successes, NFTs have also been exploited commercially. For instance, *NBA Top Shot*, with total sales exceeding \$1B [3], inspired NFT initiatives in other sports leagues [4], [5], [6] and the sportswear market, e.g., Nike's acquisition of the NFT startup RTFKT [7] (which led to *Nike CryptoKicks* [8]) and Adidas' launches of NFT ventures [9], [10]. Moreover, Starbucks' *Odyssey* [11] and Disney's *Pinnacle* [12] further signify interest in NFTs from other market sectors. To accommodate growing demand and participation, *NFT projects*, typically consisting of a limited number of unique NFTs, are distributed through online marketplaces, e.g., OpenSea [13] and Binance NFT [14].[2]

The success of NFT marketplaces hinges on effectively supporting both sellers in pricing their unique creations and buyers in discovering desirable NFTs that align with their preferences and budgets. However, NFTs exhibit unique characteristics that render conventional recommendation and pricing techniques inadequate. First, NFT transactions are transparently recorded on blockchains, allowing public access to historical pricing and ownership data, in contrast to traditional marketplaces [17], [18] that often rely on opaque or proprietary data [19]. Second, NFTs are inherently non-fungible [20] and derive value from complex trait systems [21], [22], [23], where each token carries attributes, such as color, type, rarity, and lineage, that influence both aesthetic and market value (Fig. (1)). These traits often follow predefined rarity distributions and inheritance logic, shaping user perceptions and strategic preferences. Building on this trait structure, some NFT platforms introduce interactive mechanisms for dynamic value creation, most notably *breeding* [24], [25]. Breeding allows users to combine NFTs to produce new ones, with offspring traits influenced by their digital parents (Fig. (2)). This adds a layer of strategic depth and gamification to ownership [26], creating dynamic interdependencies across the NFT ecosystem, which is an aspect not captured in traditional recommendation settings [27], [28], [29], [30].

In this paper, we formulate the *NP^{3}R (NFT Project Pricing/Purchasing Recommendation)* problem. Our approach is to model NP^{3}R as an economic game, simulating seller and buyer actions within the NFT marketplace with an aim to optimize seller revenue while simultaneously maximizing each buyer's utility of recommended NFTs. In NP^{3}R, the buyers' utility encompasses three key components: (i) the value of owning

This work is supported in part by NSF under grants III-2106758 and POSE-2346158, and in part by Academia Sinica Investigator Project Grant (AS-IV-114-M06), National Science and Technology Council (NSTC113-2221-E-001-016-MY3, NSTC112-2221-E-001-010-MY3, 114-2223-E-002-009), and Taiwan Ministry of Education (114L9009, 114L895504).

[1] Notable examples include Beeple's *"Everydays,"* sold for \$69.3M [1], and an *NBA Top Shot* of *"LeBron James Highlight,"* for \$208K [2].

[2] Beyond collectibles and branding, NFTs are also being used to support real-world asset (RWA) tokenization [15] and security token offerings (STOs) [16], enabling fractional ownership, liquidity, and verifiable provenance for physical and financial assets.

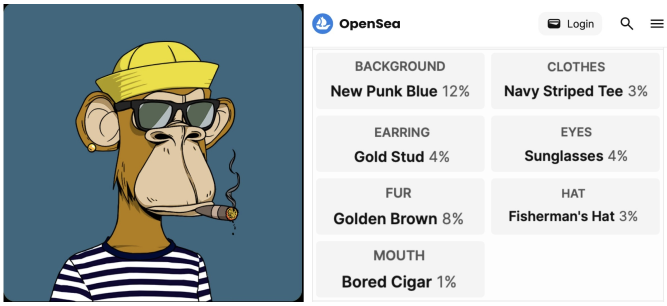

Fig. 1. *Bored Ape Yacht Club* NFT #4378 [31] and the trait descriptions of the procedurally generated digital art on the OpenSea platform [13]. The descriptions detail the NFT's attributes and their percentages, indicating the rarity of each attribute within the *Bored Ape Yacht Club* collection.

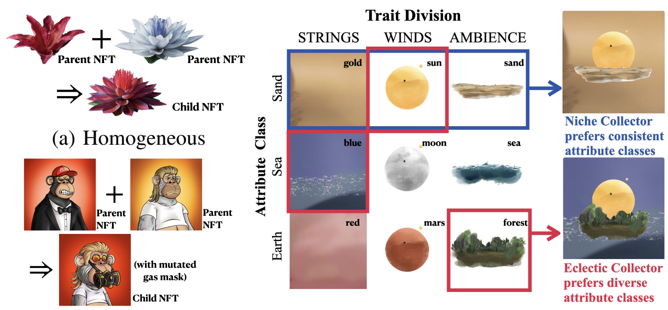

(a) Homogeneous

(b) Child-project

(c) Heterogeneous Breeding.

Fig. 2. Examples of NFT project breeding [32], [33], [34].

individual rare NFTs, (ii) the satisfaction derived from forming a personal collection, and (iii) the additional benefits of breeding, according to buyer preferences, budgets, and trait rarity. Moreover, NP^{3}R is challenging due to vast number of distinct traits and attributes, fixed supply impacting pricing strategy, and complex demand estimation due to breeding. Addressing NP^{3}R also poses significant data mining challenges, including modeling complex NFT attributes and generative relationships, and scaling algorithms for efficient recommendations. We prove that NP^{3}R is computationally hard (PPAD-complete) in Theorem 1.

To solve *NP^{3}R*, it is crucial to strike a balance between the objectives of purchasing and pricing recommendations. A focus solely on maximizing *seller revenue* may lead to buyer dissatisfaction, while prioritizing *buyer utility* could result in suboptimal revenue for the seller. These tangled considerations necessitate finding a balanced state that satisfies both parties. In other words, we need to identify an *competitive equilibrium* between the seller and the buyers, corresponding to pricing and purchasing recommendations that simultaneously yield optimal *revenue* for the seller and optimal *utility* for buyers [35], [36]. Specifically, Competitive equilibrium is achieved when the revenue-maximizing sellers and the utility-maximizing buyers are all satisfied (see Definition 10) [37]. Equipped with the above observations, we design BANTER, namely, Breeding-aware NFT Equilibrium Recommendation. BANTER leverages a dual-update iterative scheme comprising PRICE-REC and NFT-REC to achieve the *competitive equilibrium*, i.e., the optimal strategy for both the seller and the buyers, respectively (Proposition 1). NFT-REC recommends purchases to optimize buyers' utilities based on pricing derived by PRICE-REC, which then updates the prices of the next iteration based on aggregate demand of all buyers from the current NFT-REC recommendations. Crucially, Theorem 5 establishes BANTER's convergence to the competitive equilibrium, which signifies maximized buyer utilities alongside market-clearing prices that optimize seller revenue.

Central to the complexity of NP^{3}R are the diverse breeding mechanisms supported by popular NFT platforms [13], which enable the creation of new NFTs and significantly impact buyer utility and market dynamics. Understanding these mechanisms is crucial for effective recommendation. This paper considers three primary types of breeding: **1) Homogeneous Breeding** (e.g., *Axies Infinity* [38] and *Heterosis* [32] in Fig. 2((a))), which generates child NFTs from a pair of parent NFTs, is the most common type. However, it risks market saturation by inheriting the same attribute designs [39] with a *population factor* to value child NFTs with rare attributes. **2) Child-project Breeding** (e.g., *Fat Ape Club* [33] and *Roaring Leader* [40]) creates unique child NFT designs and mitigates market saturation through random mutations to improve novelty [41] (e.g., the "gold shade glasses" on the child NFT in Fig. 2((b))). **3) Heterogeneous Breeding** (e.g., *Trait Swap* [42] and *First Supper* [43]) creates customized composite artworks appealing to buyers with specific artistic objectives. It selects one NFT from each *trait division* (e.g., the horizontal categories in Fig. 2((c)) that delineate different types of images), where buyers may select an *attribute class* (e.g., the vertical categories in Fig. 2((c)) for each trait division to determine the design styles of the instances). This feature facilitates customized NFT breeding for two distinct buyer types based on their design preferences [44]: **i) niche collectors** [45], who seek consistency, can select NFTs with a uniform attribute class across trait divisions (e.g., blue box selections in Fig. 2((c))); **ii) eclectic collectors** [46], who prefer diversity, can choose from different attribute classes (e.g., red box selections in Fig. 2((c))). These mechanisms are formally defined in Section III-B.

To efficiently address the combinatorial challenge in breeding of NFT-REC, we design the *Optimal Parent Pair Selection (OPPS)* for Homogeneous Breeding and Child-project Breeding and *Heterogeneous Parent Set Selection (HPSS)* for Heterogeneous Breeding. Specifically, *OPPS* identifies optimal parent pairs for breeding by evaluating the *amalgamated valuations* (i.e., NFT's personalized value) of buyer preferences and instance rarity, while *HPSS* further curates NFT parent sets by prioritizing the parents with consistent and diverse attribute classes, preferred by niche and eclectic collectors, respectively. OPPS and HPSS improve BANTER's scalability by significantly reducing computational complexity (Theorem 2), while achieving a bounded approximation ratio (Proposition 2) and maintaining optimal breeding utility for buyers without exhaustive search after convergence.

The contributions in this work are as follows.

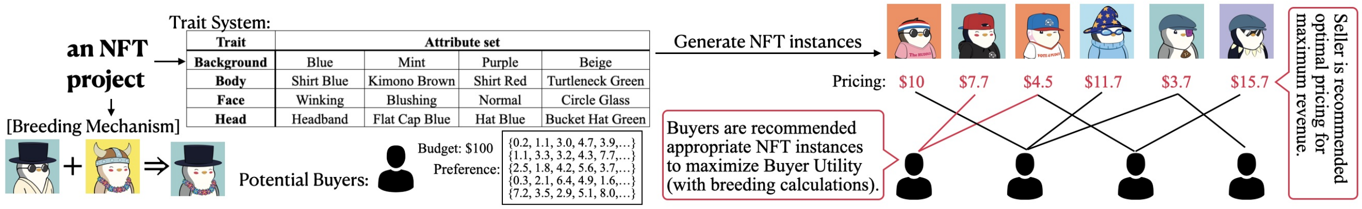

Fig. 3. Illustration of the NFT Project Pricing/Purchasing Recommendation (NP^3R) problem. The NP^3R problem involves optimizing prices for maximum seller revenue and optimizing NFT purchasing and breeding for maximum buyer utility for NFT projects comprising a *trait system* and a *breeding mechanism*.

- We formulate the NFT Project Pricing/Purchasing Recommendation (NP^3R) problem for NFTs with traits and breeding, not explored in traditional recommendations.
- We propose BANTER for NP^3R to derive optimal pricing and purchasing recommendations. To address the combinatorial challenge due to breeding, we propose *Optimal Parent Pair Selection (OPPS)* and *Heterogeneous Parent Set Selection (HPSS)* with guaranteed performance.
- Theoretical analyses prove the hardness of NP^3R and the convergence of BANTER to a competitive equilibrium.
- Extensive experiments on five real-world NFT projects show that BANTER consistently surpasses all baseline methods in revenue and average utility (with smaller runtime) across all scenarios.

II. Related Works

Blockchain and NFTs.

Recent works in blockchain technology have catalyzed various innovations, ranging from security enhancement [47], smart contracts [48], [49], to authentication [50], paving the way for diverse applications. Among them, NFTs have garnered significant attention across research fields including finance [51], [19] and cryptography [20], [52] due to their potential to revolutionize digital asset markets [53], [54]. In finance, scholars examine NFTs' impact on fintech [55], [56], [57] and marketing [58], [59], [60]. Additionally, NFTs' influence on property rights and business models is discussed across domains such as art [61], [62], [63], sports [64], [65], and entertainment [66]. Research also explores correlations of NFTs' high valuations with other assets [67], [68], [69], [70], [71], [72]. However, these studies do not consider the competitive equilibrium between sellers and buyers and also neglect the impact of breeding on buyers' utility. Another branch of NFT research focuses on security issues such as transparency [73], market manipulation [74], and NFT ownership validation [75], [76], [77], [78]. More relevant to our work are studies on NFT valuation based on internal traits or visual designs [79], [22] and external social media influences [80], [81], [82]. While insightful, they neglect the buyer demand and breeding mechanism, which are addressed in our approach. Some works address NFT recommendation [83], [84], [85], [86], [87]. However, they focus on buyer preferences based on NFT attributes but ignore breeding. Besides, they also neglect the buyers' budget constraints and the equilibrium between seller pricing and buyers' purchasing decisions, which are crucial for simultaneously optimizing both the seller revenue and the buyers' utilities.

Pricing and Purchasing Recommendation.

Existing research on pricing explores real-time bidding [88], [18], vehicle dispatch services [89], [90], [91], and seasonal pricing strategies [92]. However, these models are not designed for NFTs, which present unique challenges due to their *finite supply*. Similarly, prevalent purchasing recommendation systems primarily emphasize user preferences [93], [94], [95] and item attributes [96], usually overlooking *pricing* and breeding of new NFTs from existing NFTs. Such approaches typically employ user-item rating matrices [97], [27], enhance by social network influence [98], [99], [28], and leverage deep learning models [27], [28]. Other studies address recommendation scenarios for item bundles [100], [29] and buyer groups [101], [102], [30], [103], [104] in group recommendations. However, all the above works neglect the *competitive equilibrium* between sellers and buyers, and the interconnectedness of NFT instances due to the *trait system* and the *breeding mechanism*, which creates new NFTs from parent NFTs, not considered in traditional commodity recommendations [27], [28], [29], [30].

Classical recommendation methods fall short because they (1) ignore the critical role of breeding, and (2) treat pricing [105], [90], [92] and purchasing [27], [28] as separate tasks. As such, they cannot support the joint pricing and purchasing recommendations central to NP^3R. To our knowledge, no prior work finds competitive equilibrium to jointly optimize seller revenue and buyer utility in NFT markets. Although some studies consider social consensus [103], [104] or item bundling [29], none fully capture the unique characteristics of NFTs—such as trait systems and breeding—and their substantial impact on buyer utility (see Section III-A).

Other related topics in recommendation.

We discuss the relation of this work with other special topics in recommendations, none of which address NFT-specific challenges like breeding mechanics and trait systems. First, **fairness in recommendation** aims to prevent biased recommendations for protected groups (C-fairness) [106] or bias on how often sellers are recommended (P-fairness) [107]. However, they treat the two fairnesses independently [108], even for joint CP-fairness works [109]. In contrast, we model direct buyer-seller interactions where purchasing influences pricing and vice versa. **Multi-objective recommendation** focuses on Pareto-Efficient trade-offs between goals [110],

TABLE I
SUMMARY OF NOTATIONS.

Notations	Descriptions
$\mathcal{N}$	The set of N NFT buyers, denoted as $b_1, \ldots, b_N$.
$\mathbf{a}^i$	Trait affinity tensor of buyer b_i, consisting of T affinity vectors, $\mathbf{a}^i = (\mathbf{a}^i_1, \ldots, \mathbf{a}^i_T)$.
$\mathcal{M}$	The set of M NFT instances $\eta_1, \ldots, \eta_M$.
$\boldsymbol{\alpha}^j$	Attribute tensor of NFT instance η_j, consisting of T one-hot vectors, $\boldsymbol{\alpha}^j = (\boldsymbol{\alpha}^j_1, \ldots, \boldsymbol{\alpha}^j_T)$.
B^i, U^i, R^i	Budget, utility, and remaining budget of b_i.
$\mathcal{A}_t$	The attribute set for each trait $t \in [1, \ldots, T]$.
$\mathbf{Q}$	The supply vector. $\mathbf{Q}_j$ records the number of copies of NFT assets per NFT instance η_j.
$\mathbf{p}$	The recommended pricing ($\mathbf{p}_j$ is price of η_j).
$\mathbf{x}^i$	The recommended purchases for buyer b_i. $\mathbf{x}^i_j$ indicates the amount of η_j recommended to b_i.
$\mathcal{P}, \mathcal{L}, \mathcal{C}$	A parent NFT set, pruned list of parent NFTs, and the candidate set of parent NFT sets.
$V(\eta_j)$	The objective valuation of η_j.
$\tilde{V}^i(\eta_j)$	The amalgamated valuation of η_j for buyer b_i.
$q(\boldsymbol{\alpha}^j_t)$	The number of NFTs possessing attribute $\boldsymbol{\alpha}^j_t$.
k	The breeding count restriction.
$\mathcal{K}$	The subset of all parent NFT sets that yields the top-k breeding results.
r	The random mutation rate.
r^i_{breed}	The child breeding rate for buyer i.
f_{pop}	The population factor due to market saturation.
$q_c(\boldsymbol{\alpha}^c_t)$	The number child NFTs that possess the attribute $\boldsymbol{\alpha}^c_t$ among all child NFTs created by all buyers in Homogeneous Breeding.
$\mathbb{M}(\mathcal{P})$	The mode count that finds the attribute class with the largest number of NFT instances in the parent set $\mathcal{P}$ and returns the count of NFT instances belonging to that class.
$\mathbb{U}(\mathbf{P})$	The unique count that counts the number of unique attribute classes among $\eta \in \mathcal{P}$.
$\mathbf{z}$	The excess demand, i.e., $\sum_i \mathbf{x}^i(\mathbf{p}) - \mathbf{Q}$, the difference between the aggregate buyer purchase recommendations and the supply.
β^i	The normalized budget $B^i / \sum_i B^i$ of buyer b_i.
ϕ	A convex potential for the NP^{3}R problem.
U	The aggregated utility $U = \prod_i U^i(\mathbf{x}^i)^{\beta^i}$.

[111] but do not consider equilibrium between the seller and buyers. Similar to our work, **value-aware recommendation** [112], [113], [114] considers economic costs. However, these works only incorporate fixed pricing as a static factor in user preference, without addressing dynamic pricing based on buyer demands or considering hard budget constraints. Lastly, the **reciprocal recommendation** is markedly different from our work, involving matches between two symmetrical parties (e.g., online dating [115]). In contrast, our setting is asymmetrical, i.e., buyers select NFTs, but (the seller of) NFTs do not select buyers; the seller sets the prices of NFTs.

III. THE NP^{3}R PROBLEM

In the NP^{3}R problem, we focus on the scenario of an NFT project launch with N buyers, M NFT instances generated through a *trait system*, and a *breeding mechanism* allowing buyers to create child NFTs from their purchases. Table I summarizes the notations.

Definition 1 (Trait System)**.** *A trait system comprises T traits, where each NFT instance η_j is defined by an attribute tensor $\boldsymbol{\alpha}^j = (\boldsymbol{\alpha}^j_1, \ldots, \boldsymbol{\alpha}^j_T)$, specifying one attribute per trait. Each instance η_j has a supply of $\mathbf{Q}_j$ interchangeable copies, each referred to as an* NFT asset*.*

For instance, in Fig. 1, NFT #4378 of the BAYC digital art collection [116] comprises attributes "Gold Stud" for the "EARRING" trait and "Golden Brown" for the "FUR" trait.

Definition 2 (Breeding Mechanism)**.** *The NFT breeding mechanism enables the creation of a new child NFT, $\eta_c = \text{BREED}(\mathcal{P})$, from parent NFTs $\mathcal{P}$, under a breeding count limit of k child NFTs per buyer, which aims to prevent market oversupply in order to retain the NFT value.*[3]

In particular, existing research widely overlooks NFT trait systems [27], [28] and breeding [79], [80], [83], [86], respectively. NP^{3}R aims to find the optimal pricing recommendation to the seller and the optimal purchasing recommendation to the buyers simultaneously. As shown in Fig. 3, NP^{3}R can be divided into two subproblems: 1) *Buyer Purchasing Recommendation (BPR)*, which recommends NFT purchases to maximize the utilities of buyers according to their budgets and preferences, NFT pricing, and the breeding mechanism; 2) *Seller Pricing Recommendation (SPR)*, which optimizes pricing for maximum seller revenue. In the following, we use $\mathbf{x}^i$ to formally represent buyer b_i's purchasing recommendations under the pricing vector $\mathbf{p}$, where $\mathbf{x}^i_j$ (jth element of $\mathbf{x}^i$) is the amount of NFT η_j recommended to b_i and $\mathbf{p}_j$ (jth element of $\mathbf{p}$) is the price of η_j.

Definition 3 (The BPR problem)**.** *Given a pricing $\mathbf{p}$ and $U^i(\mathbf{x}^i)$, the utility of buyer b_i, the BPR problem aims to solve*

$$\hat{\mathbf{x}}^i = \arg\max_{\mathbf{x}^i} U^i(\mathbf{x}^i), \ \ s.t. \ \mathbf{x}^i \cdot \mathbf{p} \leq B^i, \tag{1}$$

where B^i is the budget of buyer b_i.

Definition 4 (The SPR problem)**.** *Given the NFT instance set $\mathcal{M}$ with supply vector $\mathbf{Q}$ and the buyer set $\mathcal{N}$, SPR seeks to maximize*

$$\hat{\mathbf{p}} = \arg\max_{\mathbf{p}} \sum_{\eta_j \in \mathcal{M}} \mathbf{p}_j \cdot \min\left(\mathbf{Q}_j, \sum_{b_i \in \mathcal{N}} \mathbf{x}^i_j\right) \tag{2}$$

according to the purchasing recommendation $\mathbf{x}^i$ from solving BPR, where $\min(\cdot)$ restricts total purchase from exceeding over the supply.

For instance, consider two NFTs priced at 2 and 1, respectively. For a quick idea of BPR, one may consider that a buyer spending his budget on the first NFT yields obtains a half in quantity compared to spending the same amount on the second NFT, yet the buyer's utility is derived based on the NFTs he obtains and his remaining budget (see Definition 5 later). Thus, we assume a buyer carefully optimizes his budget allocation. Moreover, for SPR, assuming that most buyers

[3]E.g., Axie Infinity [38] limits the number of breedings for each NFT.

prefer (or derive more utility from) the first NFT over the second one. If the seller sets identical prices, the first NFT is likely sold out quickly, leaving many potential buyers unable to acquire it due to limited supply, while the second NFT may remain unsold, reducing overall revenue. By updating the price to match the demand, the seller can earn more revenue.

Remark. Traditional products usually assume massive supplies. However, NFT projects inherit combinatorial pairing strategies (for breeding) yet have a fixed supply, making it challenging to find optimal pricing and purchasing. In particular, NP^{3}R differs from prior recommendation scenarios in three key ways: 1) the fixed supply of NFTs makes pricing crucial for optimizing revenue; 2) pricing and purchasing are interdependent, requiring a competitive equilibrium; 3) the breeding mechanism in NFTs which introduces additional complexity (detailed in Section III-B): while buyers gain additional utility from breeding new NFTs, they must optimize parent set combinations under different breeding mechanisms, and the seller must anticipate demand shifts driven by buyers' breeding decisions. These are new challenges absent in existing recommendation frameworks.

Applications. NP^{3}R is formulated for NFT marketplaces (e.g., Opensea [13], Binance NFT [14]) to support users of NFT projects. However, by ignoring the breeding utility, NP^{3}R also supports traditional scenarios such as travel packages, crowdsourcing, concert ticketing, talent recruitment, umbrella fundraising, etc. For instance, by treating travel destinations as NFTs, where attributes are the activities and supply are the available spots.

The hardness of NP^{3}R is presented as follows.

Theorem 1. *The NP^{3}R problem for M instances and N buyers with budgets is PPAD-complete.*[4]

Proof. We reformulate the NP^{3}R problem by considering buyers as active players in a Nash game. In particular, we consider a buyer's spending strategy to *divide* his budget among $M+1$ slots, where one slot is reserved for withholding budget, while the other M slots correspond to budgets dedicated to each of the M instances. Such a scheme satisfies the budget constraint for each buyer. Furthermore, by setting the price of each instance η_j to $Q_j / \sum_i a_j^i B^i$, where a_j^i denotes the budget portion committed by buyer b_i to NFT instance η_j, we can obtain a price vector that also satisfies the supply limit $\mathbf{Q}$ (see Definition 4). Since the ratios of $M+1$ slots sum up to 1, the division scheme corresponds to a mixed strategy profile between the $M+1$ actions, where each value is the probability of taking the corresponding action. Thus, the equilibrium problem can be formulated as a Nash game in which each buyer has $M+1$ actions. Furthermore, the competitive equilibrium corresponds to the Nash equilibrium since each buyer obtains his maximum utility at the competitive equilibrium and cannot do better by unilaterally changing his budget allocations. By [117], the complexity of obtaining the Nash equilibrium is PPAD-complete. Thus, the NP^{3}R problem is also PPAD-complete. $\square$

[4] PPAD-completeness entails the inherent and extreme computational difficulty associated with resolving equilibria, which makes attaining their efficient resolution challenging in both game-theoretical and economic models [117].

As shown, the joint optimization of BPR and SPR presents significant computational challenges. A buyer's decision space spans M dimensions, corresponding to potential budget allocations across M NFT instances, and the sheer scale and combinatorial complexity of the joint action space for these N buyers are primary drivers of the problem's PPAD-completeness. Therefore, our strategy is to find the competitive equilibrium between buyers and sellers [118] by individually deriving the optimal solutions of BPR and SPR to iteratively update the pricing and the purchasing recommendations.

A. Buyer's Utility

Following the literature on buyer behaviors [119], [120] and NFT valuation [79], we introduce key components of buyer utility in the NFT market. Beyond the value of money (represented by the *remaining budget* R^i) [121], a buyer b_i's utility comprises 1) *Instance-wise NFT utility* (U^i_{Instance}), representing the objective value of individual NFTs, primarily determined by their rarity within the market [22]; 2) *Collection-based NFT utility* ($U^i_{\mathit{Collection}}$), capturing the subjective appreciation derived from owning a set of NFTs, considering the interrelationships and collective attributes of the NFTs in a buyer's portfolio [119]; and 3) *NFT breeding utility* (U^i_{Breeding}), accounting for the potential value of child NFTs generated via the breeding mechanism [122], [123]. Existing recommendation systems, however, largely overlook such multifaceted NFT utility, particularly the value derived from breeding and collections [27], [124], [86], [87].

Definition 5 (Buyer's Utility)**.** *The buyer's utility U^i for b_i is*

$$U^i(\mathbf{x}^i) \equiv U^i_{\mathit{Instance}}(\mathbf{x}^i) + U^i_{\mathit{Collection}}(\mathbf{x}^i) + U^i_{\mathit{Breeding}}(\mathbf{x}^i) + R^i, \quad (3)$$

where R^i is the remaining budget of buyer b_i.

In the following, we model the three components of the buyer utility.

a) Instance-wise NFT Utility (U^i_{Instance}): As observed in multiple studies [79], [22], [125], [126], an NFT's value is significantly influenced by the *rarity* of its attributes, due to the non-fungible property of NFTs. This observation is reinforced by the prevalence of rarity statistics for popular NFT projects, which buyers routinely consult to make informed purchasing decisions [127], [128], [129]. To capture this crucial aspect, we formulate the Instance-wise NFT utility U^i_{Instance} as

$$U^i_{\mathit{Instance}}(\mathbf{x}^i) \equiv \sum_{\eta_j \in \mathcal{M}} \mathbf{x}^i_j V(\eta_j), \; V(\eta_j) = \sum_{t=1}^{T} \log\left(\frac{|\mathbf{Q}|}{q(\boldsymbol{\alpha}^j_t)}\right), \quad (4)$$

where $V(\eta_j)$ is the *objective valuation* of NFT instance η_j taking into account of rarity. Following Mekacher et al. [22], we adopt an occurrence frequency-based valuation model, where $q(\boldsymbol{\alpha}^j_t)$ denotes the number of NFTs with attribute $\boldsymbol{\alpha}^j_t$, and $|\mathbf{Q}|$ is the total number of NFTs. Thus, we can capture the inverse relationship between attribute frequency and NFT value. Note that in the context of NFTs, the non-fungible property introduces a constraint of supply limit $\mathbf{Q}$. In contrast, traditional item recommendations usually do not discuss the case where items are sold out. Specifically, the non-fungible property ensures rarity; without it, NFTs can be duplicated, collapsing their objective value V as the quantity explodes.

b) Collection-based NFT Utility ($U^i_{Collection}$): Next, based on consumer behavior studies in the NFT market [130], [131], [132], we recognize that collectors also derive utility from curating personal NFT portfolios, influenced by individual preferences for specific NFT attributes and the synergy between attributes to form a collection.[5] Indeed, real-world NFT marketplaces support attribute-based searches and offers, allowing collectors to search for the ideal attributes required for their personalized collections [137], [138], [139]. To capture these aspects, we formulate the Collection-based NFT utility $U^i_{Collection}$ as

$$U^i_{Collection}(\mathbf{x}^i) \equiv \sum_{t=1}^{T} \mathbf{a}^i_t \cdot \log\left(\sum_{\eta_j \in \mathcal{M}} \mathbf{x}^i_j \boldsymbol{\alpha}^j_t + \mathbf{1}\right), \qquad (5)$$

where $\mathbf{a}^i_t$ is the *trait affinity tensor* recording buyer b_i's preferences for each trait attribute t, and the logarithm is applied element-wise to the vector sum plus the all-one vector $\mathbf{1}$. In other words, $U^i_{Collection}$ models the utility of viewing all NFTs in the buyer's possession as a collection of diverse attributes, where the sum of these attributes experiences diminishing returns [140] via a logarithmic function and is weighted by the buyer preferences [141], [142].

c) NFT Breeding Utility ($U^i_{Breeding}$): Finally, we model the NFTs breeding utility, a unique feature that significantly separates NFTs from conventional assets, not considered in existing recommendations [27], [28]. According to the idea of fractional NFTs [143], [144], wherein an NFT is segmented into smaller fractions to make it more accessible to a broader base of potential purchasers, we introduce the child breeding rate $r^i_{breed}(\mathcal{P})$, which represents the amount of child NFTs generated by combining the parent set $\mathcal{P}$ with fractional parent NFTs [145], [146]. The child breeding rate is defined as follows.

$$r^i_{breed}(\mathcal{P}) \equiv \frac{1}{|\mathcal{P}|} \sum_{\eta_j \in \mathcal{P}} \min(1, \mathbf{x}^i_j), \qquad (6)$$

where the contribution of each parent NFT to child breeding rate is proportional to its ownership. By incorporating r^i_{breed} in the breeding utility, buyers are motivated to increase their holdings for ideal NFTs suitable for breeding.

Definition 6. *The NFT breeding utility is defined as*

$$U^i_{Breeding} \equiv \max_{\mathcal{K}^i \subset \mathcal{S}} \sum_{\mathcal{P} \in \mathcal{K}^i} r^i_{breed}(\mathcal{P}) \mathbb{V}^{i,\text{TYPE}}[\mathcal{P}], \qquad (7)$$

where $\mathcal{K}^i$ is a subset of all parent combinations $\mathcal{S}$ whose total child breeding rate $\sum_{\mathcal{P} \in \mathcal{K}^i} r^i_{breed}(\mathcal{P})$ is within the breeding count limit k (Definition 2). $\mathbb{V}^{i,\text{TYPE}}[\mathcal{P}]$ is buyer b_i's expected value of a child NFT from parent set $\mathcal{P}$ under different breeding types ("homo," "child," "niche," "eclectic"), defined later in Definitions 7 to 9.

Example. As shown in Fig. 2, different breeding mechanisms yield distinct results. Homogeneous Breeding (Fig. 2((a))) blends parental traits for refined value, while Child-project Breeding (Fig. 2((b))) introduces mutations (e.g., unique glasses) for novelty and rarity. Heterogeneous Breeding (Fig. 2((c))) further create composites from uniform attribute classes (e.g., 'Sand') for thematic consistency appealing to *niche* collectors, or from varied classes for *eclectic* collectors.

B. The Expected Value Functions for Breedings

To account for market saturation from duplicated NFT attributes in Homogeneous Breeding, we adopt the *population factor* $f_{pop}(\eta_c) = \sum_{t=1}^{T} \exp\left(-\frac{q(\boldsymbol{\alpha}^c_t)}{|\mathbf{Q}|}\right)$, following [22]. Here, $f_{pop}(\eta_c)$ considers each attribute $\boldsymbol{\alpha}^c_t$ of child NFT η_c, where $q(\boldsymbol{\alpha}^c_t)$ is the number of NFTs with $\boldsymbol{\alpha}^c_t$, and $|\mathbf{Q}|$ is the total NFT count. Furthermore, we introduce the buyer's amalgamated valuation [22], [79], $\tilde{V}^i(\eta) = \left(\sum_t \mathbf{a}^i_t \cdot \boldsymbol{\alpha}_t\right) V(\eta)$, tailoring the objective valuation of $V(\eta)$ by buyer preferences.[6].

Definition 7. $\mathbb{V}^{i,homo}$ *for Homogeneous Breeding is*

$$\mathbb{V}^{i,homo}[\mathcal{P}] \equiv \mathbb{E}\left[f_{pop}(\eta_c)\tilde{V}^i(\eta_c)\right], \eta_c = \text{BREED}(\mathcal{P}), \qquad (8)$$

where $\tilde{V}^i$ is the amalgamated valuation, and each child attribute $\boldsymbol{\alpha}^c_t$ is inherited from parent p_1 or p_2 (from $\mathcal{P}$) with equal probability.

Example. In Fig. 2((a)), the child NFT inherits the red color and the flower shape from each of its parent NFTs, respectively. Considering a parent set $\mathcal{P} = (\eta_1, \eta_2)$, if all attributes are different between η_1 and η_2 (i.e., $\alpha^1_t \neq \alpha^2_t,\ \forall t$), then the expectation value $\mathbb{V}^{i,homo}(\mathcal{P})$ is calculated over all 2^T possible child NFT attributes, weighted by the population factor estimated by the attribute distribution of all buyers' parent NFT selections.[7]

Definition 8. $\mathbb{V}^{i,child}$ *for Child-project Breeding is*

$$\mathbb{V}^{i,child}[\mathcal{P}] \equiv \mathbb{E}\left[\tilde{V}^i(\eta_c)\right], \eta_c = \text{CHILD-BREED}(\mathcal{P}, r), \qquad (9)$$

where CHILD-BREED *creates η_c such that each attribute $\boldsymbol{\alpha}^c_t$ is assigned $\boldsymbol{\alpha}^{p_1}_t$ or $\boldsymbol{\alpha}^{p_2}_t$ (from $\mathcal{P}$) with probability $(1-r)/2$ each;[8] otherwise, $\boldsymbol{\alpha}^c_t$ is randomly assigned an attribute from $\mathcal{A}_t$ with mutation probability r for each trait t.[9]*

Example. In Fig. 2((b)), the child NFT inherits "Tank Top" and "Red" (background) from its parent NFTs, while gaining a "golden sunglass" attribute from random mutation of r.

[5]For instance, NFT collectors can display their NFTs in the metaverse [133], i.e., virtual galleries such as Spatial [134] and Voxels (formerly Cryptovoxels) [135], [136].

[6]Amalgamated valuation reflects an NFT's personalized worth to a buyer, adjusting its objective value with a "personalization factor" that quantifies that specific buyer's preference for the NFT's attributes

[7]Random sampling is leveraged for approximate estimations in practice.

[8]Following *CryptoKitties* [41], r is predefined by the sellers.

[9]Child-project Breeding set all $f_{pop} = 1$ as it addresses market saturation by creating unique child NFT designs and through mutation (with r) that can introduce rare attributes not found in parent NFTs.

Considering a parent set $\mathcal{P} = (\eta_1, \eta_2)$, the child NFT resulting from Child-project Breeding has probability r of obtaining a new attribute not found in η_1 and η_2.

Finally, Heterogeneous Breeding incorporates *trait divisions* and *attribute classes* to categorize NFT instances. This structure allows buyers to select one parent NFT from each *trait division*, considering *attribute classes* to guide design style choices, with the distinct preferences of *niche* and *eclectic* collectors requiring separate functions.

Definition 9. *In Heterogeneous Breeding, the parent NFT set $\mathcal{P}$ consists of NFT instances from each of the D trait divisions, with $|\mathcal{P}| = D$. For niche collectors, the expected value is*

$$\mathbb{V}^{i,niche}[\mathcal{P}] = \mathbb{M}(\mathcal{P}) \sum_{\eta \in \mathcal{P}} \tilde{V}^i(\eta), \tag{10}$$

where $\mathbb{M}(\mathcal{P}) \equiv \max_c |\{\eta \in \mathcal{P} \mid class(\eta) = c\}|$ returns the count of NFTs in the most frequent attribute class c within $\mathcal{P}$, and $\tilde{V}$ is the amalgamated valuation. For eclectic collectors,

$$\mathbb{V}^{i,eclectic}[\mathcal{P}] = \mathbb{U}(\mathcal{P}) \sum_{\eta \in \mathcal{P}} \tilde{V}^i(\eta), \tag{11}$$

where $\mathbb{U}(\mathcal{P}) \equiv |\{c \mid \exists \eta \in \mathcal{P}, class(\eta) = c\}|$ counts the distinct attribute classes among $\eta \in \mathcal{P}$.

Here, $\mathbb{M}$ is a *majority count* [147] favoring the majority attribute class in $\mathcal{P}$, suiting *niche* collectors who prefer consistent breeding designs. Conversely, the *diversity count* $\mathbb{U}$ favors attribute class variety in $\mathcal{P}$, supporting *eclectic* collectors' preference for diverse designs [148]. This dual expectation definition under Heterogeneous Breeding underscores the need for customized recommendations for specific buyer preferences.

Example. In Fig. 2((c)), the example child NFT for niche collectors (blue boxes) is a composite artwork comprising parent NFTs all from the "Sand" attribute class, while the example child NFT for eclectic collectors (red boxes) is a composite artwork comprising diverse parent NFTs from all three attribute class. Considering a parent set $\mathcal{P}$ consists of three NFTs from different attribute classes c_1, c_2, c_3, the *mode count* $\mathbb{M}(\mathcal{P}) = 1$ is small while the *diversity count* $\mathbb{U}(\mathcal{P}) = 3$, indicating that breeding with a diverse parent set suits eclectic collectors more than niche collectors.

Remark. For clarity, the core novelty of this formulation lies in modeling the multifaceted utility specific to NFTs, introducing concepts largely absent in traditional commodity recommendation. These include utility derived from NFT attribute rarity (U^i_{Instance}), collection synergy ($U^i_{\mathit{Collection}}$), and especially NFT breeding (U^i_{Breeding}). This breeding component alone necessitates unique considerations such as breed rates (r^i_{breed}), expected child values across different breeding types ($\mathbb{V}^{i,\text{TYPE}}$), population saturation factors (f_{pop}), and personalized amalgamated valuations ($\tilde{V}^i$). Importantly, our framework is modular and adaptable: by setting the breeding utility $U^i_{\mathit{Breeding}} = 0$, it reduces to a general combinatorial preference model, retaining expressiveness across domains. For example, $U^i_{\mathit{Collection}}$ captures synergies in travel bundles, while U^i_{Instance} reflects seat or artist preferences in ticketing. In crowdsourcing, it models task-skill fit and task set value; in fundraising, milestone-based benefits map to compositional utility. These examples highlight the framework's flexibility in capturing both additive and interaction-based preferences.

IV. BANTER

We present *BANTER*, Breeding-aware NFT Equilibrium Recommendation, an iterative algorithm featuring dual recommendation components: pricing (PRICE-REC) and NFT purchasing with breeding (NFT-REC), to address NP^{3}R. BANTER models NP^{3}R as an economic game, simulating seller and buyer actions within the NFT marketplace. The target outcome is a competitive equilibrium, a state that simultaneously achieves optimal buyer utility and seller revenue [149].

Definition 10. *A competitive equilibrium is a strategy profile $(\mathbf{p}^*, \mathbf{x}^{i*})$ where i) $\mathbf{p}^*$ is the optimal pricing that solves the SPR problem, and ii) $\mathbf{x}^{i*}$ is the optimal purchasing for each buyer b_i that solves the BPR problem, given $\mathbf{p}^*$.*

Example. Given a pricing $\mathbf{p}$, each buyer b_i can separately optimize their purchasing strategy $\mathbf{x}^{i*}$ within the budget constraint. However, the pricing may not be optimal for the seller. In particular, the supply may be less than the aggregate demand from the buyers, indicating that some buyers are unable to obtain their desired NFTs and that the seller could have set a higher price to gain more revenue. Conversely, if the price is set too high, buyers may be unwilling to purchase NFTs because the obtained NFTs do not yield NFT-based utilities comparable to simply keeping the budget unspent (i.e., the remaining budget utility R).

The interdependence between the seller's pricing and buyers' purchasing decisions means that changes in one affect the other's optimal response, making iterative updates necessary for reaching equilibrium. Crucially, we show that this competitive equilibrium is obtained at the *market-clearing condition* [150], [151], where total supply matches aggregate demand, ensuring full allocation without surplus or shortage.

Proposition 1. *A market-clearing condition is the joint recommendations $\{\tilde{\mathbf{p}}, \tilde{\mathbf{x}}\}$ where*

$$\forall b_i \in \mathcal{N} : \tilde{\mathbf{x}}^i = \underset{\mathbf{x}^i \cdot \tilde{\mathbf{p}} \le B^i}{\arg\max}\, U^i(\mathbf{x}^i)\ ,\ s.t.\ \forall j : \sum_{i=1}^{N} \tilde{\mathbf{x}}^i_j = \mathbf{Q}_j, \tag{12}$$

establishes a competitive equilibrium.

Proof. First, since $\tilde{\mathbf{x}}^i$ maximizes b_i's utility under the pricing $\tilde{\mathbf{p}}$, it represents the optimal purchasing decision for the buyer b_i. Next, we need to show that $\tilde{\mathbf{p}}$ maximizes the seller's revenue given the buyers' optimal responses. We prove this by contradiction. Let $\mathbf{p}'$ be a pricing with corresponding buyer recommendations $\mathbf{x}'^i$ that is not in market clearing but maximizes seller revenue. Since $\mathbf{p}'$ is not in market clearing, the recommendations deviate from the supply constraint $\sum_i \mathbf{x}'^i_j \neq \mathbf{Q}_j$ for some NFT instance η_j. For an NFT instance η_j with $\sum_i \mathbf{x}'^i_j > \mathbf{Q}_j$, the price $\mathbf{p}'_j$ is too low and could be raised until a corresponding $\sum_i \mathbf{x}'^i_j = \mathbf{Q}_j$. By

Algorithm 1 The BANTER method.

Input: Budgets $\{B^i\}$, affinity tensors $\{\mathbf{a}^i\}$, attribute tensors $\{\boldsymbol{\alpha}^j\}$ supply vector $\mathbf{Q}$, step-size ϵ, parameters K_{init}, K, K_d. Candidate set length K_c. $\textsc{type}(i)$ is the breeding and collector type of b_i.

$\mathbf{p} \leftarrow \textsc{init}(K_{init}, \{\mathbf{a}^i\}, \{\boldsymbol{\alpha}^j\}, \{B^i\}, \mathbf{Q})$
for K iterations **do**
  for $i = 1$ **to** N **do**
    $\mathbf{x}^i \leftarrow$NFT-REC $(K_d, \mathbf{a}^i, \{\boldsymbol{\alpha}^j\}, B^i, \mathbf{p}, K_c, \textsc{type}(i))$
  $\epsilon, \mathbf{p} \leftarrow$PRICE-REC $(\epsilon, \mathbf{p}, \{\mathbf{x}^i\}, \mathbf{Q})$
procedure $\textsc{init}(K_{init}, \{\mathbf{a}^i\}, \{\boldsymbol{\alpha}^j\}, \{B^i\}, \mathbf{Q})$
  random initialize $\mathbf{p}$
  for K_{init} iterations **do**
    $\forall i, j : \mathbf{s}^i_j \leftarrow \sum_t \mathbf{a}^i_t \boldsymbol{\alpha}^j_t / \mathbf{p}_j$
    $\forall j : \mathbf{p}_j \leftarrow \left(\sum_i B^i \cdot \frac{\mathbf{s}^i_j}{\sum_j \mathbf{s}^i_j} \right) / \mathbf{Q}_j$
  return $\mathbf{p}$

Algorithm 2 The NFT-REC procedure for a buyer b_i.

procedure NFT-REC$(K_d, \mathbf{a}^i, \{\boldsymbol{\alpha}^j\}, B^i, \mathbf{p}, K_c, \textsc{type})$
  random init $|\mathbf{s}^i| = 1$, $\forall j : \mathbf{x}^i_j \leftarrow (\mathbf{s}^i_j B^i)/\mathbf{p}_j$
  for K_d iterations **do**
    $U^i_{\textit{Instance}} \leftarrow \sum_j \mathbf{x}^i_j \cdot V(\boldsymbol{\alpha}^j)$
    $U^i_{\textit{Collection}} \leftarrow \sum_t \mathbf{a}^i_t \cdot \log \left(\sum_j \mathbf{x}^i_j \boldsymbol{\alpha}^j_t + 1 \right)$
    $U^i_{\textit{Breeding}} \leftarrow \textsc{breeding-utility}(\mathbf{x}^i, K_c, \textsc{type})$
    $U^i \leftarrow U^i_{\textit{Instance}} + U^i_{\textit{Collection}} + U^i_{\textit{Breeding}} + B^i \mathbf{s}^i_{-1}$
    $\mathbf{s}^i \leftarrow \left(\mathbf{s}^i + \epsilon_s \frac{\partial U^i}{\partial \mathbf{s}} \right)$
    $\mathbf{s}^i \leftarrow \frac{\mathbf{s}^i}{|\mathbf{s}^i|}$
    $\forall j : \mathbf{x}^i_j \leftarrow (\mathbf{s}^i_j B^i)/\mathbf{p}_j$
  return $\mathbf{x}^i$

Definition 4, increasing the price strictly improves the revenue, since the quantity term is capped at $\mathbf{Q}_j$. For an NFT instance η_j with $\sum_i \mathbf{x}'^i_j < \mathbf{Q}_j$, the price $\mathbf{p}'_j$ is too high. Focusing on the logarithmic form of the NFT collection utility and the remaining budget term R in U^i (Equation (3)), we find $U^i(\mathbf{p}_j) = C \log(\mathbf{x}'^i_j + 1) + B^i - \mathbf{x}'^i_j \mathbf{p}_j$, where C is a scalar constant. Using the optimal condition of $\mathbf{x}'^i_j$, $\partial U^i / \partial \mathbf{x}'^i_j = 0$, we find $C/(\mathbf{x}'^i_j + 1) - \mathbf{p}_j = 0$. Thus, $\mathbf{x}'^i_j = C/\mathbf{p}_j - 1$ and the revenue from η_j is $\mathbf{x}'^i_j \mathbf{p}_j = C - \mathbf{p}_j$. Thus, revenue increases as prices fall. Considering $U^i_{\textit{Instance}}$ andn $U^i_{\textit{Breeding}}$, the solution $\mathbf{x}'^i_j$ would become greater than what is derived above, since the additional Instance and Breeding utilities would further compel more purchases from buyers. Thus, the seller can potentially increase their revenue by lowering prices to encourage more purchases, up to the point where the demand meets the supply. Note that lowering the price only increases revenue up to the market clearing point, as further decreasing the price results in $\sum_i \mathbf{x}'^i_j > \mathbf{Q}_j$, where the earlier analysis should be applied. Therefore, the market clearing pricing $\tilde{\mathbf{p}}$ obtains the maximum revenue for the seller. □

The connection between the market-clearing condition and competitive equilibrium provides the theoretical foundation for BANTER. By designing our algorithm to attain NFT market clearing, we solve NP^{3}R with two main components (Algorithm 1). PRICE-REC refines pricing (to solve SPR) by

Algorithm 3 The PRICE-REC procedure.

procedure PRICE-REC$(\epsilon, \mathbf{p}, \{\mathbf{x}^i\}, \mathbf{Q})$
  $\mathbf{z} \leftarrow \sum_i \mathbf{x}^i - \mathbf{Q}$
  $\epsilon \leftarrow \epsilon \exp \left(\gamma \frac{\|\mathbf{z}\|_2}{\|\mathbf{Q}\|_2} \right)$
  $\mathbf{p} \leftarrow \mathbf{p} \left(1 + \epsilon \frac{\mathbf{z}}{|\mathbf{z}|} \right)$

i) adjusting prices of high-demand NFT instances after buyer recommendations from NFT-REC, and ii) designing a *demand-aware* step-size schedule to accelerate convergence. NFT-REC then finds optimal buyer purchases (to solve BPR) by i) recommending NFTs based on the updated pricing from PRICE-REC, and ii) selecting appropriate breeding combinations. The adaptive interaction between PRICE-REC and NFT-REC ensures that BANTER converges to market clearing, as proven in Theorem 5. Moreover, to speed up convergence, we design INIT for BANTER to establish initial preference-aware prices, thereby providing a more refined starting point for BANTER's main iterative process, by iteratively improving them over K_{init} iterations, based on buyer preferences ($\mathbf{a}^i$) and NFT attributes ($\boldsymbol{\alpha}^j$). Afterward, BANTER alternates between improving pricing (via PRICE-REC) and purchasing recommendations (via NFT-REC) to progressively converge towards equilibrium. To efficiently manage the complex breeding utility calculations within NFT-REC, BANTER also employs specialized pruning schemes, i.e, *Optimal Parent Pair Selection (OPPS)* for Homogeneous Breeding and Child-project Breeding, and *Heterogeneous Parent Set Selection (HPSS)* for Heterogeneous Breeding. These schemes identify high-potential parent NFTs by considering buyer preferences, attribute rarity, and buyer collection styles (*niche* or *eclectic*), thereby significantly reducing the cost of exploring all possible breeding options.[10]

A. *The* NFT-REC *Procedure*

Given a pricing $\mathbf{p}$ obtained in the previous iteration of PRICE-REC, NFT-REC solves BPR by finding the optimal purchase recommendation $\mathbf{x}^i$ for each buyer b_i that maximizes their individual utility U^i (Equation (3)). As detailed in Algorithm 2, NFT-REC first introduces an expenditure proportion vector $\mathbf{s}^i \in [0,1]^{M+1}$ for each buyer b_i, normalized with its element sum as one (i.e., $\sum_k \mathbf{s}^i_k = 1$). Each element $\mathbf{s}^i_j$ (for $j \neq -1$) represents the fraction of budget B^i allocated to purchase NFT instance η_j, while a special element $\mathbf{s}^i_{-1}$ represents the fraction of the budget to be retained ($R^i \equiv \mathbf{s}^i_{-1} B^i$). Based on $\mathbf{s}^i$, the recommended purchase quantity is $\mathbf{x}^i_j \equiv B^i \mathbf{s}^i_j / \mathbf{p}_j$ for NFT η_j.

NFT-REC iteratively refines $\mathbf{s}^i$ over many iterations. In each iteration, it calculates the instance-wise ($U^i_{\textit{Instance}}$) and collection-based ($U^i_{\textit{Collection}}$) utility components using the current $\mathbf{x}^i$. It then derives the breeding utility ($U^i_{\textit{Breeding}}$) according to the BREEDING-UTILITY procedure (Section IV-C),

[10]We present ablation tests in Section VI-D to validate our design choices by ablating key components (e.g., INIT, demand-aware step-size scheduling, OPPS/HPSS pruning logic).

Algorithm 4 The BREEDING-UTILITY calculation.

procedure BREEDING-UTILITY($\mathbf{x}^i, K_c$, TYPE)
  if TYPE **is** homo **or** child **then**
    $\mathcal{C} \leftarrow$ OPPS (i, K_c)
  if TYPE **is** niche **or** eclectic **then**
    $\mathcal{C} \leftarrow$ HPSS (i, K_c)
  $c_{breed} \leftarrow 0$
  $U^i_{Breeding} \leftarrow 0$
  for $\mathcal{P}$ **in** $\mathcal{C}$ **do**
    $r_{breed} \leftarrow \frac{1}{|\mathcal{P}|} \sum_{\eta_j \in \mathcal{P}} \min(\mathbf{x}^i_j, 1)$
    $c_{breed} \leftarrow c_{breed} + r_{breed}$
    $U^i_{Breeding} \leftarrow U^i_{Breeding} + r^i_{breed} \mathbb{V}^{i,\text{TYPE}}[\mathcal{P}]$
    if $c_{breed} \geq k$ **then break**
  return $U^i_{Breeding}$

Algorithm 5 OPPS (Optimal Parent Pair Selection)

procedure OPPS(i, K_c)
  $\mathcal{L} \leftarrow$ top K_c instances from $\mathcal{M}$ **sorted by** $f_{pop}(\eta_j)\tilde{V}^i(\eta_j)$
  $\mathcal{C} \leftarrow \{(\eta_p, \eta_q) \mid \eta_p, \eta_q \in \mathcal{L}, \eta_p \neq \eta_q\}$
  sort $\mathcal{C}$ **by** $\frac{1}{2} \sum_{\eta \in \mathcal{P}} f_{pop}(\eta_p)\tilde{V}^i(\eta)$
  return $\mathcal{C}$

which carefully examines diverse breeding configurations. To improve the total utility U^i, $\mathbf{s}^i$ is updated using gradient ascent with respect to U^i and then re-normalized (L1-norm) to maintain in budget. Through this iterative refinement of $\mathbf{s}^i$ and the corresponding derivation of $\mathbf{x}^i$, NFT-REC aims to maximize each buyer's utility U^i while inherently adhering to their budget B^i. In contrast to NFT-REC, traditional commodity recommendation systems do not incorporate dynamic pricing into purchase suggestions [27], [124], [96] and, as they are designed for non-generative items, inherently omit considerations of NFT-specific breeding [27], [124], [96], [97], [95].

B. *The* PRICE-REC *Procedure*

In each iteration t, PRICE-REC improves the pricing $\mathbf{p}^t$ by

$$\mathbf{p}^{t+1} = \mathbf{p}^t \left(1 + \epsilon^t \frac{\mathbf{z}}{\|\mathbf{z}\|_2}\right), \ \mathbf{z} \equiv \sum_i \mathbf{x}^i(\mathbf{p}^t) - \mathbf{Q}, \qquad (13)$$

where $\mathbf{z}$ is the *excess demand*, i.e., the difference between the sum of $\mathbf{x}$ (recommendation from NFT-REC) and $\mathbf{Q}$. In particular, prices are raised for NFT η_j when $\mathbf{z}_j > 0$ and vice versa. To expedite convergence, we design an adaptive *demand-aware* scheduling,

$$\epsilon^t = \epsilon^{t-1} \exp\left(\frac{\|\mathbf{z}\|_2}{\|\mathbf{Q}\|_2}\right), \qquad (14)$$

where ϵ^{t-1} is the step size in the previous iteration. Intuitively, we increase the step size when the overall market imbalance (i.e., the normalized magnitude of total excess demand, $\frac{\|\mathbf{z}\|_2}{\|\mathbf{Q}\|_2}$) becomes substantial to support a more imminent and decisive price adjustment to rapidly correct significant demand-supply disparities and thereby expedite convergence towards equilibrium.

Algorithm 6 HPSS (Heterogeneous Parent Set Selection)

procedure HPSS(i, K_c)
  Initialize $\mathcal{C}$ as an empty set.
  $\mathcal{L} \leftarrow$ top K_c instances from $\mathcal{M}$ **sorted by** $\tilde{V}^i(\eta_j)$
  for η_j **in** $\mathcal{L}$ **do**
    $\mathcal{P} \leftarrow \{\eta_j\}$
    for k **from** j **to** K_c **do**
      if $trait\_division(\eta_k)$ **not in** $\mathcal{P}$ **then**
        $\mathcal{P}$ **append** η_k
      if $|\mathcal{P}| = D$ **then**
        $\mathcal{C}$ **append** $\mathcal{P}$
        break
  $\mathbb{F} \equiv \mathbb{M}$ **if** b_i **is** niche collector **else** $\mathbb{F} \equiv \mathbb{U}$
  sort $\mathcal{C}$ **by** $\mathbb{F}(\mathcal{P}) \sum_{\eta \in \mathcal{P}} \tilde{V}^i(\mathcal{P})$
  return $\mathcal{C}$

C. *The* BREEDING-UTILITY *Improvement*

Optimizing $U^i_{Breeding}$ by brute-force examination of all parent combinations $\mathcal{P}$ in BREEDING-UTILITY (Algorithm 4) is computationally prohibitive. To enhance scalability, we design *Optimal Parent Pair Selection (OPPS)* (Algorithm 5) for Homogeneous Breeding and Child-project Breeding, and *Heterogeneous Parent Set Selection (HPSS)* (Algorithm 6) for Heterogeneous Breeding. OPPS and HPSS identify a candidate set $\mathcal{C}$ of promising parent NFT sets by selectively evaluating preferences across various breeding and buyer types to reduce computational overhead.

Specifically, since $U^i_{Breeding}$ (Definition 6) prioritizes high-value parent combinations, pruning less valuable pairs from the search space is important. Parent candidates are first sorted for each buyer to evaluate the influence of buyer-specific preferences ($\tilde{V}^i$) on breeding utility. OPPS ranks NFTs by $f_{pop}(\eta_j)\tilde{V}^i(\eta_j)$ for Homogeneous Breeding and by $\tilde{V}^i(\eta_j)$ for Child-project Breeding, selecting the top K_c for a candidate list $\mathcal{L}$ to reduce the search space. According to f_{pop}, it yields a competitor-aware list prioritizing rarer outcomes. Candidate set $\mathcal{C}$ then includes all parent pairs $\mathcal{P}$ formed from $\mathcal{L}$, ranked by their combined $\tilde{V}^i(\eta_p) + \tilde{V}^i(\eta_q)$.

For Heterogeneous Breeding, HPSS selects the top-K_c list $\mathcal{L}$ from $\mathcal{M}$ based on $\tilde{V}^i$. Parent sets $\mathcal{P} \in \mathcal{C}$ are formed by selecting one parent from $\mathcal{L}$ and completing the set with others from $\mathcal{L}$ to carefully include all trait divisions. These sets $\mathcal{P}$ are then ranked by attribute class consistency ($\mathbb{M}(\mathcal{P})$) or diversity ($\mathbb{U}(\mathcal{P})$) to suit niche or eclectic collectors, respectively (Definition 9), identifying high-value, tailored parent sets to effectively accelerate BANTER's convergence (Proposition 2).

From candidate set $\mathcal{C}$, an optimal subset $\mathcal{K}^i \subseteq \mathcal{C}$ is chosen for buyer b_i. $\mathcal{K}^i$ maximizes $\sum_{\mathcal{P} \in \mathcal{K}^i} r^i_{breed}(\mathcal{P}) \mathbb{V}^{i,\text{TYPE}}[\mathcal{P}]$ with the total breeding rate $\sum_{\mathcal{P} \in \mathcal{K}^i} r^i_{breed}(\mathcal{P}) \leq k$ (the breeding count limit). The selection involves iteratively adding parent pairs from the ranked candidate set $\mathcal{C}$ to $\mathcal{K}^i$, ensuring the total breeding rate remains within the limit k. For efficient calculation of $f_{pop}(\eta_c)$ used in $\mathbb{V}^{i,homo}$ for Homogeneous Breeding (dependent on global child attribute counts $q(\boldsymbol{\alpha}^c_t)$), we exploit a hash map to track processed parent sets per buyer. Global attribute counts $q(\boldsymbol{\alpha}^c_t)$ are updated by aggregating

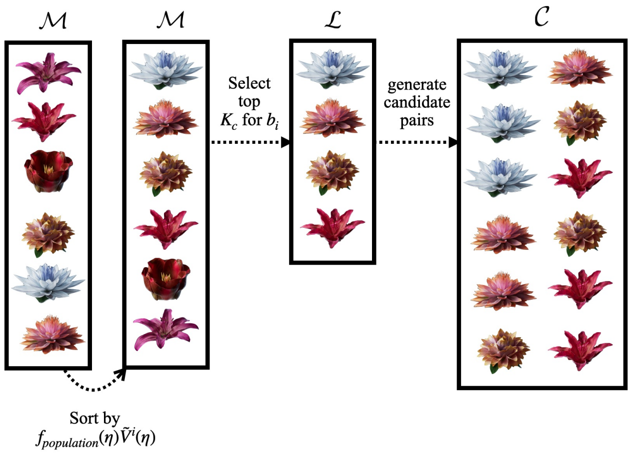

Fig. 4. Illustration of OPPS in the BREEDING-UTILITY procedure with the *Heterosis* project (also presented in Fig. 2((a))). OPPS selects the top K_c NFT instances to form $\mathcal{L}$, then forms the candidate set $\mathcal{C}$ by pairing NFT instances in $\mathcal{L}$. Without OPPS, the candidate set would increase to $M(M-1)/2$, where M is the number of NFT instances. Thus, OPPS reduces the search space by focusing on the most promising parent pairs $\mathcal{P}$ to generate child NFTs. The resulting candidate set $\mathcal{C}$ is further sorted following step 4 of Algorithm 5.

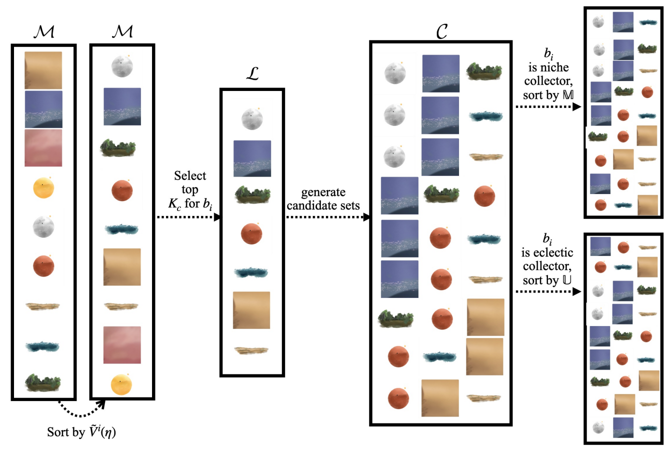

Fig. 5. Illustration of HPSS in the BREEDING-UTILITY procedure with the *Pann* project (also presented in Fig. 2((c))). HPSS selects the top K_c NFT instances to form $\mathcal{L}$, then forms the candidate set $\mathcal{C}$ by iteratively taking an NFT instance as the first instance in $\mathcal{P}$ and choosing subsequent NFT instances from $\mathcal{L}$ to form the parent set $\mathcal{P}$, consisting of one NFT instance from each trait division. Without OPPS, the candidate set would increase to the order of $(M/D)^D$, where M is the number of NFT instances and D is the number of trait divisions. Thus, HPSS trims the search space by focusing on the most promising parent sets $\mathcal{P}$ to generate child NFTs while following the mechanism of Heterogeneous Breeding. The resulting candidate set $\mathcal{C}$ is further sorted following step 10 of Algorithm 6.

anticipated child attributes from all buyers' current breeding decisions (weighted by their $r^i_{breed}(\mathcal{P})$).

The overall complexity reduction of BANTER by OPPS and HPSS is presented as follows.

Theorem 2. *By applying OPPS under Homogeneous Breeding and Child-project Breeding, BANTER's time complexity is reduced from $O(KNM^2)$ to $O(KN|\mathcal{C}|)$, where K is the iteration count, $|\mathcal{C}|$ is the constant candidate set length, and N, M, and D is the number of buyers, NFT instances, and trait divisions, respectively. Similarly, applying HPSS under Heterogeneous Breeding lowers the time complexity from $O(KNM^D)$ to $O(KN|\mathcal{C}|)$.*

Proof. In Algorithm 1, the NFT-REC procedure is called KN times, where K is a constant iteration number while N is the number of buyers. Under Homogeneous Breeding and Child-project Breeding, the NFT-REC must consider all possible parent NFT pairs to calculate the NFT breeding utility in the order of $O(M^2)$, where M is the number of NFT instances. Under Heterogeneous Breeding, assuming D trait divisions evenly distribute M NFT instances, all possible parent NFT sets are in the order of $O(M^D)$. By utilizing OPPS or HPSS, the considered NFTs parent sets are reduced from M^2 or M^D to the constant length of the candidate set $|\mathcal{C}|$. Thus, the time complexity of BANTER becomes $O(KN|\mathcal{C}|)$. □

D. Illustrations for OPPS and HPSS

Figs. 4 and 5 provide illustrative examples for OPPS and HPSS using the *Pann* project, respectively, while Fig. 6 showcases the trait divisions, attribute classes, and NFT instance names within the *Pann* project. As shown in Fig. 4, for buyer b_i, OPPS first ranks $\mathcal{M}$ by $f_{pop}(\eta)\tilde{V}^i(\eta)$ and selects the top K_c NFT instances to form the candidate list $\mathcal{L}$. Then, it forms the candidate set $\mathcal{C}$ by pairing NFT instances in $\mathcal{L}$. This process trims the search space by focusing on the most promising parent pairs $\mathcal{P}$ for generating child NFTs. For instance, in Fig. 4, based on the sorted candidate list $\mathcal{L}$, the top parent candidate pairs consisting of the first (blue flower) and second (pink flower) NFTs are placed at the top.

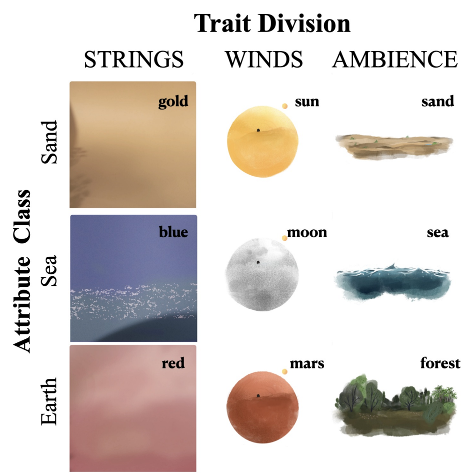

Fig. 6. Trait divisions, attribute classes, and names of individual NFT instances in the Pann [34] project.

On the other hand, as illustrated in Fig. 5 with trait divisions and attribute classes detailed in Fig. 6, HPSS selects the top K_c NFT instances to form the set $\mathcal{L}$ based on $\tilde{V}^i(\eta)$. It then constructs the candidate set $\mathcal{C}$ by iteratively choosing an NFT instance as the initial element in the parent set $\mathcal{P}$ and subsequently selecting additional NFT instances from $\mathcal{L}$.

Each parent set $\mathcal{P}$ consists of one NFT instance from each trait division. Concretely, in Fig. 5, HPSS initially selects "moon" from the "WINDS" trait division, then proceeds to select "blue" from the "STRINGS" division and "sea" from the "AMBIENCE" division, while skipping "mars," another instance from the "WINDS" division. The resulting parent set of "moon," "blue," and "sea" thus occupies the first position in the candidate set $\mathcal{C}$. Note that the naming of these NFT instances is detailed in Fig. 6. Once $\mathcal{C}$ is fully constructed, HPSS ranks the parent sets based on either the consistency or diversity of attribute classes, catering to niche or eclectic collectors, respectively. For instance, the parent set consisting of "moon," "blue," and "sea" all belong to the "Sea" attribute class, making it more appealing to niche collectors while less so to eclectic collectors. Thus, after sorting by $\mathbb{M}$, the NFT parent set consisting of "moon," "blue," and "sea" is raised to the top of the candidate sets for b_i as a niche collector, since all three NFTs belong to the same attribute class "Sea." In contrast, after sorting by $\mathbb{U}$, the NFT parent set consisting of "blue," "mars," and "sand" is raised to the top of the candidate sets for b_i as an eclectic collector, since all three NFTs belong to different attribute classes. By sorting the parent sets according to the buyer's preferences, we ensure that the pruned candidate set can still be approximately optimal.

V. Theoretical Analysis

Here, we prove that BANTER converges to the competitive equilibrium for NP^{3}R, where the equilibrium is connected to the market clearing condition based on Proposition 1.

BANTER's convergence is proven by a) leveraging an aggregate utility to ensure the resulting allocation is optimal for every individual buyer (Theorem 3), b) establishing an excess demand potential function whose gradient provides a clear, computable signal for adjusting prices towards market-clearing (Theorem 4), and c) using this gradient scheme to guarantee the iterative process reaches a stable competitive equilibrium (Theorem 5). This framework is designed to be comprehensive, as the buyer utility that underpins this entire analysis explicitly incorporates the nuanced values derived from NFT breeding.

To further ensure efficient convergence, we design the demand-aware step-size scheduling (Equation (14)). Intuitively, PRICE-REC adjusts prices inversely to excess demand z (Equation (13)), encouraging NFT-REC to reduce purchase demand for over-demanded NFTs and vice versa. Thus, each iteration naturally progresses towards the market clearing condition, with careful step-size scheduling that progressively reducing the step sizes to avoid overshooting. In particular, we verify that BANTER converges with the acceleration of demand-aware scheduling in the ablation study in Section VI-D.

A. Aggregated Utility

We first prove that an optimal solution for an aggregated utility U aligns with the optimal solution for $U^i(\mathbf{x}^i)$ of each buyer b_i. The aggregated utility is defined as follows.

$$U \equiv \prod_i U^i(\mathbf{x}^i)^{\beta^i} \text{ , and } \beta^i \equiv B^i / \sum_i B^i, \tag{15}$$

where the exponent β^i is the normalized budget, which will become a scalar weight when U is log-transformed. It finds the following solution

$$\bar{\mathbf{x}}^1, \ldots, \bar{\mathbf{x}}^N \in \underset{\mathbf{x}^1,\ldots,\mathbf{x}^N}{\arg\max}\, U,\ s.t. \sum_i \mathbf{x}^i \leq \mathbf{Q}. \tag{16}$$

Theorem 3. *Assuming U^i (and thus U) are concave, homogeneous, continuous, and non-decreasing utility functions, the aggregated solution $\bar{\mathbf{x}}^i$ to Equation (16) is an optimal solution to Equation (12).*

Proof. First, note that $\sum_i \bar{\mathbf{x}}^i = \mathbf{Q}$. Otherwise, we may add the remaining supply to any buyer and obtain a larger U as it is non-decreasing. We use the mathematical properties of homogeneous functions presented in [152], [153]. In particular, due to the duality in homogeneous function programming [153], if $\{\bar{\mathbf{x}}^i\}_{i=1}^N \in \arg\max_{\sum_i \mathbf{x}^i \leq \mathbf{Q}} U$, there exists $\mathbf{q} \in \mathbb{R}^M$ such that

$$\sum_i \bar{\mathbf{x}}^i \cdot \mathbf{q} = \mathbf{Q} \cdot \mathbf{q} = \prod_i U^i(\bar{\mathbf{x}}^i)^{\beta^i} \tag{17}$$

and

$$\sum_i \mathbf{x}^i \cdot \mathbf{q} \geq \prod_i U^i(\mathbf{x}^i)^{\beta^i} \tag{18}$$

for any $\mathbf{x}^i$. Divide both sides of Equation (18) by the last two terms of Equation (17) respectively, we obtain

$$\sum_i \mathbf{x}^i \cdot \boldsymbol{\rho} \geq \prod_i \left(\frac{U^i(\mathbf{x}^i)}{U^i(\bar{\mathbf{x}}^i)}\right)^{\beta^i}, \tag{19}$$

where $\boldsymbol{\rho} = \frac{\mathbf{q}}{\mathbf{Q}\cdot\mathbf{q}}$. Consider the case where only buyer k deviates from the aggregated solution, i.e., $\mathbf{x}^i = \bar{\mathbf{x}}^i, i \neq k$ and denote buyer k's allocation as $\mathbf{x}^k$. Then

$$\sum_i \mathbf{x}^i \cdot \boldsymbol{\rho} = \mathbf{Q} \cdot \boldsymbol{\rho} - (\bar{\mathbf{x}}^k - \mathbf{x}^k) \cdot \boldsymbol{\rho} \geq \left(\frac{U^k(\mathbf{x}^k)}{U^k(\bar{\mathbf{x}}^k)}\right)^{\beta^k} \tag{20}$$

We now utilize the homogeneous property of U^k. In particular, suppose that $\mathbf{x}^k = \lambda \bar{\mathbf{x}}^k$ for some scalar λ, since by the definition of $\boldsymbol{\rho}$, $\mathbf{Q}\cdot\boldsymbol{\rho} = 1$, we have $\boldsymbol{\rho}\cdot\bar{\mathbf{x}}^k(\lambda-1) \geq \lambda^{\beta^k} - 1$ by Equation (20). By taking the limit of λ approaching 1 from positive to negative, we find

$$\boldsymbol{\rho} \cdot \bar{\mathbf{x}}^k = \lim_{\lambda \to 1} \frac{1-\lambda^{\beta^k}}{1-\lambda} = \beta^k \tag{21}$$

In other words, $\boldsymbol{\rho}$ can be considered as the corresponding price vector for the solution $\bar{\mathbf{x}}$. However, since $\sum_i \bar{\mathbf{x}}^i \cdot \boldsymbol{\rho} = \mathbf{Q} \cdot \boldsymbol{\rho} = 1$, by Equation (20), any $\mathbf{x}^k$ that satisfies the budget constraint $\mathbf{x}^k \cdot \boldsymbol{\rho} = \beta^k$ finds $\left(\frac{U^k(\mathbf{x}^k)}{U^k(\bar{\mathbf{x}}^k)}\right)^{\beta^k} \leq 1$, and thus $U^k(\mathbf{x}^k) \leq U^k(\bar{\mathbf{x}}^k)$, implying that the buyer k can not improve his own utilities by deviating from the aggregated solution. The theorem follows. $\square$

B. Excess Demand Potential

To assess the deviation from equilibrium before convergence, we introduce the excess demand potential ϕ using the Lagrangian of $\log U = \sum_i \beta_i \log U^i(\mathbf{x}^i)$, where $\log$ is applied for a simplified representation [36], [118]. The optimization problem of $\log U$ under the supply constraint (Equation (12)) yields the Lagrangian formulation below.

$$\mathscr{L}(\{\mathbf{x}^i\}, \mathbf{p}) \equiv \sum_i \beta^i \log U^i(\mathbf{x}^i) - \sum_j \mathbf{p}_j (\sum_i \mathbf{x}^i_j - \mathbf{Q}_j), \quad (22)$$

where $\mathbf{p}_j$ is the Lagrangian multipliers corresponding to the price of item j. Based on the Lagrangian $\mathscr{L}$, the potential function becomes

$$\phi \equiv \max_{\{\mathbf{x}^i\}} \mathscr{L}(\{\mathbf{x}^i\}, \mathbf{p}). \quad (23)$$

Theorem 4 (Convexity and gradient of ϕ)**.** *ϕ defined in Equation (23) is convex and $\nabla\phi = -\mathbf{z}$, where $\mathbf{z}$ is defined in Equation (13).*

Proof. First, we observe that ϕ is convex by the construction of Equation (22). Second, since $\mathscr{L}$ is the Lagrangian of the aggregated utility, $\arg\max_{\{\mathbf{x}^i\}} \mathscr{L}(\{\mathbf{x}^i\}, \mathbf{p})$ optimizes the aggregated utility U. Thus, by Theorem 3, it is also the demand allocation that maximizes individual utilities U^i. However, since the potential ϕ is defined as the maximum of many linear functions (with regard to $\mathbf{p}$), the gradient is given by taking the $\arg\max$ of $\mathbf{x}$ [36]. Thus, by Equation (22) and (23), we have

$$\nabla\phi = -\left(\sum_i \arg\max_{\mathbf{x}^i} U^i(\mathbf{x}^i) - \mathbf{Q}\right) \equiv -\mathbf{z}. \quad (24)$$

The theorem follows. □

C. Gradient Descent Convergence Analysis

Given the excess demand potential ϕ, BANTER exploits the gradient descent to converge to the competitive equilibrium.

Theorem 5. *Denote $\mathbf{p}^* \equiv \arg\min_{\mathbf{p}} \phi(\mathbf{p})$ as the minimizer of the convex potential ϕ, and the optimal $\phi^* \equiv \phi(\mathbf{p}^*)$. Assume $\nabla\phi$ is L- Lipschitz continuous and step-size $\epsilon \leq \frac{2}{L}$. For any starting point $\mathbf{p}^0$, $\lim_{t\to\infty} \phi(\mathbf{p}^t) = \phi^*$.*

Proof. We follow [154] to derive the proof. We first observe that the distance $\|\mathbf{p}^t - \mathbf{p}^*\|^2$ is non-increasing with respect to t.

$$\begin{aligned}&\|\mathbf{p}^{t+1} - \mathbf{p}^*\|^2 \\ &= \|\mathbf{p}^t - \mathbf{p}^*\|^2 - 2\epsilon\nabla\phi(\mathbf{p}^t)\cdot(\mathbf{p}^t - \mathbf{p}^*) + \epsilon^2\|\nabla\phi(\mathbf{p}^t)\|^2 \\ &\leq \|\mathbf{p}^t - \mathbf{p}^*\|^2 - \epsilon(2/L - \epsilon)\|\nabla\phi(\mathbf{p}^t)\|^2,\end{aligned} \quad (25)$$

where the L-Lipschitz condition is applied to the middle term to obtain the inequality. Next, we leverage the basic assumptions on ϕ to find $\nabla\phi(\mathbf{p}^t)(\mathbf{p}^{t+1} - \mathbf{p}^t) \leq \phi(\mathbf{p}^{t+1}) - \phi(\mathbf{p}^t) \leq \frac{L}{2}\|\mathbf{p}^{t+1} - \mathbf{p}^t\|^2$, where the first inequality holds due to convexity while the second inequality is due to L-Lipschitzness. Rearranging the terms and applying L-Lipschitzness to connect the norm distance term and the gradient term again, we find

$$\phi(\mathbf{p}^{t+1}) \leq \phi(\mathbf{p}^t) - \epsilon(1 - \epsilon L/2)\|\nabla\phi(\mathbf{p}^t)\|^2. \quad (26)$$

Again, by convexity, $\phi(\mathbf{p}^t) - \phi^* \leq \nabla\phi(\mathbf{p}^t)\cdot(\mathbf{p}^t - \mathbf{p}^*)$. However, since the distance $\|\mathbf{p}^t - \mathbf{p}^*\|$ is decreasing, we may find the following bound.

$$\phi(\mathbf{p}^t) - \phi^* \leq \|\nabla\phi(\mathbf{p}^t)\|\|\mathbf{p}^0 - \mathbf{p}^*\| \quad (27)$$

Therefore, applying Equation (26) for the difference between consecutive ϕ values onto Equation (27), we find the following inequality bound.

$$\begin{aligned}\phi(\mathbf{p}^{t+1}) - \phi^* &\leq \phi(\mathbf{p}^t) - \phi^* - \epsilon(1 - \epsilon L/2)\|\nabla\phi(\mathbf{p}^t)\|^2 \\ &\leq \phi(\mathbf{p}^t) - \phi^* - \epsilon(1 - \epsilon L/2)\frac{(\phi(\mathbf{p}^t) - \phi^*)^2}{\|\mathbf{p}^0 - \mathbf{p}^*\|^2},\end{aligned} \quad (28)$$

where the second inequality utilized Equation (27) again. Denoting $\Delta^t \equiv \phi(\mathbf{p}^t) - \phi^*$, we find

$$\frac{1}{\Delta^{t+1}} \geq \frac{1}{\Delta^t} + \frac{\Delta^t}{\Delta^{t+1}}\frac{\epsilon(1 - \epsilon L/2)}{\|\mathbf{p}^0 - \mathbf{p}^*\|^2} \geq \frac{1}{\Delta^t} + \frac{\epsilon(1 - \epsilon L/2)}{\|\mathbf{p}^0 - \mathbf{p}^*\|^2}. \quad (29)$$

Summing up the inequalities starting from $t = 0$, we find $\frac{1}{\Delta^{t+1}} \geq \frac{1}{\Delta^0} + (t+1)\frac{\epsilon(1-\epsilon L/2)}{\|\mathbf{p}^0 - \mathbf{p}^*\|^2}$. Thus,

$$\lim_{t\to\infty} \phi(\mathbf{p}^t) - \phi^* = 0 \quad (30)$$

The theorem follows. □

Proposition 2. *The pruning schemes OPPS and HPSS aim to effectively approximate equilibrium breeding utility. The inequality: $\frac{\sum_{\eta_j\in\mathcal{L}} V(\eta_j)}{\sum_{\eta_j\in\mathcal{M}} V(\eta_j)} \leq \left(\frac{K_c}{M}\right)^{1-1/\alpha}$ holds, where $K_c = |\mathcal{L}|$ and $M = |\mathcal{M}|$.*

Proof. First, to model the typically long-tail distribution of breeding utility contributions, we assume that the amalgamated values $\tilde{V}^i(\eta)$ of NFTs for the buyer b_i follow a Pareto distribution with sharpness α [155], a common model for long-tail distributions [156]. The Pareto distribution is defined by the PDF as follows.

$$f(v) = \frac{\alpha v_m^\alpha}{v^{\alpha+1}}, \quad v \geq v_m, \quad (31)$$

where $\alpha > 0$ is the shape parameter, and $v_m > 0$ is the minimum possible value of $\tilde{V}^i(\eta)$. The CDF becomes,

$$F(v) = 1 - \left(\frac{v_m}{v}\right)^\alpha. \quad (32)$$

The expected value exists only if $\alpha > 1$, i.e., long tail, and is given by

$$\mathbb{E}[\tilde{V}^i] = \frac{\alpha v_m}{\alpha - 1}. \quad (33)$$

Since we rank the NFTs in $\mathcal{M}$ in decreasing order of their values, we have

$$\tilde{V}^i(\eta_1) \geq \tilde{V}^i(\eta_2) \geq \cdots \geq \tilde{V}^i(\eta_{|M|}) \quad (34)$$

Our goal is to find how much of the total value is captured by the top K_c NFTs and how the approximation error ϵ depends on K_c. Using the Pareto distribution, the j-th largest value $\tilde{V}^i(\eta_j)$ can be approximated using the order statistics of the distribution. The j-th order statistic for large M is

$$\tilde{V}^i(\eta_j) \approx v_m \left(\frac{M}{j}\right)^{1/\alpha}. \quad (35)$$

Then, the total value is

$$S_{\text{total}} = \sum_{j=1}^{|M|} V_i(\eta_j) \approx \sum_{j=1}^{|M|} v_m \left(\frac{|M|}{j}\right)^{1/\alpha}. \tag{36}$$

Similarly, the cumulative value of the top K_c NFTs is

$$S_{K_c} = \sum_{j=1}^{K_c} V_i(\eta_j) \approx \sum_{j=1}^{K_c} v_m \left(\frac{|M|}{j}\right)^{1/\alpha}. \tag{37}$$

For large $|M|$ and K_c, we can approximate the sums using integrals,

$$\begin{aligned}
S_{\text{total}} \approx& \int_1^{|M|} v_m \left(\frac{|M|}{x}\right)^{1/\alpha} dx \\
=& v_m |M|^{1/\alpha} \int_1^{|M|} x^{-1/\alpha} dx \\
=& v_m |M|^{1/\alpha} \left(\frac{|M|^{1-1/\alpha} - 1}{1 - 1/\alpha}\right) \\
=& v_m \frac{|M| - |M|^{1/\alpha}}{1 - 1/\alpha}.
\end{aligned}$$

Similarity,

$$\begin{aligned}
S_{K_c} \approx& v_m |M|^{1/\alpha} \left[\frac{x^{1-1/\alpha}}{1 - 1/\alpha}\right]_{x=1}^{x=K_c} \\
=& v_m |M|^{1/\alpha} \left(\frac{K_c^{1-1/\alpha} - 1}{1 - 1/\alpha}\right).
\end{aligned}$$

Therefore, the relative error becomes $\epsilon = \frac{S_{\text{total}} - S_{K_c}}{S_{\text{total}}}$, which can be derived as follows.

$$\frac{S_{K_c}}{S_{\text{total}}} \approx \frac{v_m |M|^{1/\alpha} \left(\frac{K_c^{1-1/\alpha} - 1}{1 - 1/\alpha}\right)}{v_m \frac{|M| - |M|^{1/\alpha}}{1 - 1/\alpha}} = \frac{|M|^{1/\alpha}\left(K_c^{1-1/\alpha} - 1\right)}{|M| - |M|^{1/\alpha}}. \tag{38}$$

For large $|M|$, since $|M| \gg |M|^{1/\alpha}$, we have $|M| - |M|^{1/\alpha} \approx |M|$, and $|M|^{1/\alpha}\left(K_c^{1-1/\alpha} - 1\right) \approx |M|^{1/\alpha} K_c^{1-1/\alpha}$. Thus,

$$\epsilon \approx 1 - \frac{|M|^{1/\alpha} K_c^{1-1/\alpha}}{|M|} = 1 - \frac{K_c^{1-1/\alpha}}{|M|^{1-1/\alpha}}. \tag{39}$$

Since $|M|$ is large, $|M|^{1-1/\alpha}$ is large, and ϵ decreases as K_c increases. Finally, we have

$$\epsilon \approx 1 - \left(\frac{K_c}{|M|}\right)^{1-1/\alpha}, \tag{40}$$

leading to the approximation ratio $1 - \epsilon \approx \left(\frac{K_c}{|M|}\right)^{1-1/\alpha}$.

By selecting K_c such that $K_c/|M|$ is a small fraction but K_c is large enough, we can make ϵ arbitrarily small. Specifically, for a given $\delta > 0$, we can choose K_c such that,

$$\epsilon \leq \delta \quad \Longrightarrow \quad \left(\frac{K_c}{|M|}\right)^{1-1/\alpha} \geq 1 - \delta. \tag{41}$$

Solving for K_c,

$$K_c \geq |M|(1-\delta)^{\frac{\alpha}{\alpha-1}}. \tag{42}$$

TABLE II

DATASET STATISTICS. N DENOTES THE NUMBER OF BUYERS, M DENOTES THE NUMBER OF NFT INSTANCES, '# ASSET' DENOTES THE NUMBER OF NFT ASSETS, '# ATTR.' DENOTES THE NUMBER OF ATTRIBUTES, AND '# TRADE' DENOTES THE NUMBER OF TRANSACTIONS.

NFT project	N	M	# asset	# attr.	# trade
Axies Infinity	5515	26739	203954	288	35217
Bored Ape Yacht Club	4483	8141	8141	308	21560
Crypto Kitties	1869	5984	8465	224	7534
Fat Ape Club	4540	5189	5189	228	7726
Roaring Leader	2407	4962	4962	539	7358

Therefore, the pruning approaches OPPS and HPSS effectively approximate the optimal breeding utility by selecting the top K_c NFTs, with the approximation error ϵ. The proposition follows.

□

As will be shown in Section VI-B, BANTER converges quickly due to 1) the design of the demand-aware step-size scheduling, which adapts to the magnitude of the excess demand (Equation (14)), 2) the design of INIT for the pricing vector that provides a favorable starting point, and 3) the designs of OPPS and HPSS. To improve computational efficiency, our pruning schemes OPPS and HPSS prioritize the most promising parent breeding combinations into a smaller, more manageable set $\mathcal{L}$. This effectively trims the search space from the full candidate pool $\mathcal{M}$ by omitting combinations anticipated to yield lower breeding utility. Proposition 2 then quantifies the quality of this approximation for the breeding utility calculated in each iteration. Equipped with this bounded and step-wise approximation for breeding choices, BANTER ultimately converges to a competitive equilibrium (as proven in Theorem 5) because its gradient-based iterative updates consistently minimize the overall excess demand potential ϕ derived from these buyer decisions.

VI. EXPERIMENTS

A. Setup

a) Dataset: Table II summarizes the statistics of five real-world NFT projects on the Ethereum blockchain. Each project's trait systems and trade records, up to November 17, 2023, are collected from OpenSea [13] using the Moralis Python SDK [157].

- *Axie Infinity* [38] employs its NFT assets as characters and uses breeding to generate new characters.
- *Bored Ape Yacht Club (BAYC)* [158], featuring unique Bored Ape visual designs (see Fig. 1), is one of the most popular NFT projects.
- *Crypto Kitties* [159] is an NFT collection entertainment featuring cat designs that first introduces and encourages NFT breeding. It presents detailed and innovative breeding rules to encourage users to engage in the breeding process to obtain rare attributes.
- *Fat Ape Club* [33] features the Child-project Breeding with the *Fat Ape Babies Club* [160] (see Fig. 7).

Fig. 7. *Fat Ape Club* NFT #4360 and *Fat Ape Babies Club* NFT #2085 both have the "Laser" attribute for the "Eyes" trait, but features distinct designs. Under Homogeneous Breeding, the child NFT would continue to feature the same "Laser" design on the left. In contrast, with Child-project Breeding, the child NFT would feature the new design on the right.

- *Roaring Leaders* [40] is an NFT project featuring NFT breedings for fantasy feline arts.

We document each NFT project's trait system and compile the attribute composition of each NFT instance within the project. For *Axie Infinity*, *Crypto Kitties* and *Roaring Leaders*, we focus on the appearance traits (e.g., ears, mouth, tail) and filter out the entertainment traits (e.g., speed or attack) that have a continuous range of selections for attributes. For *Bored Ape Yacht Club* and *Fat Ape Club*, we directly use the traits and attributes designed for the trait system. For Heterogeneous Breeding, we equally split the buyers between niche and eclectic collectors, and assign NFT instances to one of three trait divisions and one of three attribute classes according to [34].

Note that we identify buyers by their blockchain addresses, filter out those with five or fewer NFT purchases, and exclude NFT instances without a trading history [28], [161]. The budget is calculated by summing the transaction prices of a buyer's purchases, while preferences are mined using [162] based on the traits in the acquired NFTs.

b) Baseline: We compare BANTER with the following baseline recommendation methods.

HetRecSys [28], [163], LightGCN [27], [164], NCF [165], Group [166], [167], Auction [168], and Greedy

- HetRecSys [28] leverages a Heterogeneous Graph Neural Network (GNN) to learn a heterogeneous graph of user preferences (user-item interactions), social networks (user-user interactions, and item graph (item-item interactions).
- LightGCN [27] leverages a lightweight Graph Convolutional Network (GCN) to model the user-item interactions.
- NCF [165] leverages fully connected layers to jointly process user and item embeddings and directly output a prediction score. Group [166] recommends the same set of items to a group of users by reaching a consensus while considering the preference of each user.
- Auction [168] simulates an auction where buyers bid on NFTs based on utility-to-price ratio. A dual-price system sets a price range, and in each round, a buyer bids on the NFT offering the best value. The process escalates prices for lower-priced NFTs, optimizing pricing recommendations for sellers.
- Greedy recommends NFTs with the highest value-to-price ratio (i.e., "*bang per buck*" [118]) with the amalgamated valuation for each buyer.

Besides Auction, we adapt baseline approaches for NP^{3}R to recommend prices and quantities. Following [126], we implement a default pricing strategy where each NFT's price is set proportionally to its objective valuation. For purchasing, we select the top-k ($k = 20$) items from baseline recommendations and optimize a uniform quantity across all selected items, subject to buyers' budget constraints. It is worth noting that this implementation enhances the baseline methods by extending their item ranking recommendations with optimized purchasing quantities. For HetRecSys, LightGCN, and NCF, we model buyers as users and NFTs as items, forming the user-user, user-item, and item-item interactions based on similarities between buyer preferences and NFT attributes. We customize Group by grouping buyers based on preference similarity.

c) Evaluation and Parameter Settings: While the baselines do not account for breeding in their recommendations, we rigorously evaluate all methods under Homogeneous Breeding, Child-project Breeding, and Heterogeneous Breeding separately. Specifically, based on the pricing and purchasing recommendations from each method, buyers are randomly sequenced to complete their purchases while adhering to both the NFT supply constraints and individual buyer budgets.

For each buyer, we first verify if the supply limit has been exceeded. For NFTs that are sold out, we mask them and ignore their recommendations, adjusting the buyer's recommendations to align with the remaining supply if necessary. Next, if the total cost of the recommended purchases exceeds the buyer's budget, we uniformly scale down the purchasing quantities to fit within the budget. After satisfying both constraints, the transaction is completed, and we record the revenue and buyer utility based on the adjusted quantities.

For Heterogeneous Breeding, each NFT instance is designated to a trait division and a attribute class following a uniform distribution, and each buyer is randomly set as a niche collector or an eclectic collector. For BANTER, we set all iteration numbers (K, K_{init}, K_d) to 128, (initial) step size $\epsilon = 1000, \epsilon_s = 1$, candidate length $K_C = 50$, mutation rate $r = 0.03$, breeding count $k = 10$. All experiments are conducted on an HP DL580 server with an Intel 2.10GHz CPU, 1TB RAM, and NVIDIA RTX 2070 GPU.

B. Experimental Results

We compare the performance of revenue (top), average buyer utility (middle), and runtime (bottom) for the three breeding mechanisms in Fig. 8. Across all metrics, BANTER consistently demonstrates superior performance, achieving the highest seller revenues and the highest average buyer utility, while incurring a low runtime. This performance improvement is attributed to BANTER's joint optimization of pricing for the

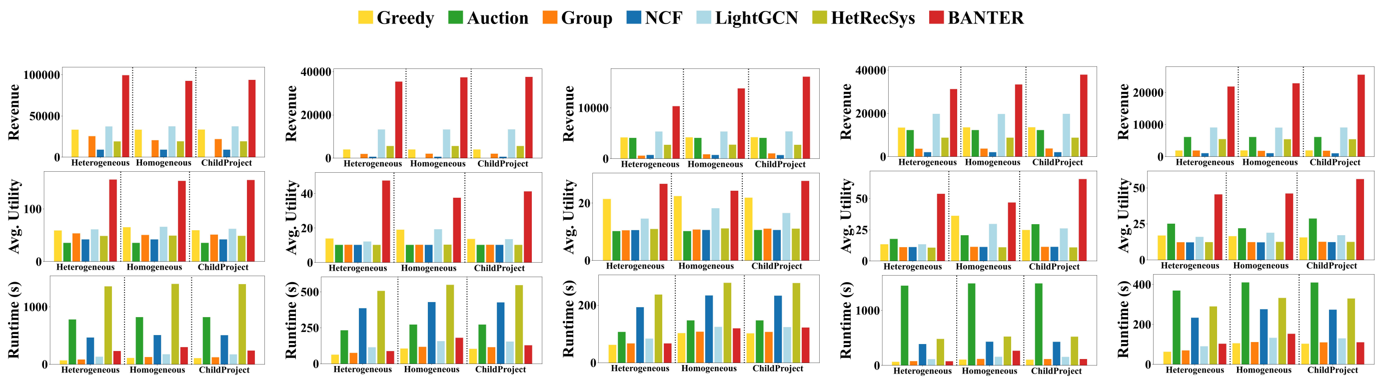

(a) *Axie Infinity* (b) *Bored Ape Yacht Club* (c) *Crypto Kitties* (d) *Fat Ape Club* (e) *Roaring Leader*

Fig. 8. Seller's revenue (top row), average buyers' utility (middle row), and runtime (bottom row) comparisons.

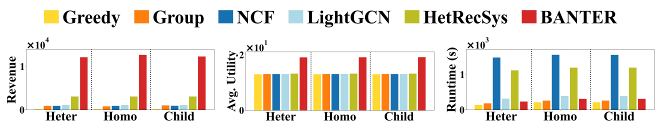

Fig. 9. Seller's revenue (left), average buyers' utility (middle), and runtime (right) on the Yelp dataset.

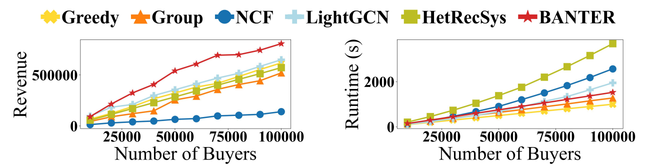

Fig. 10. Scalability test on large number of buyers.

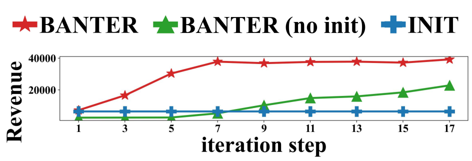

Fig. 11. Ablation tests over initial iteration steps.

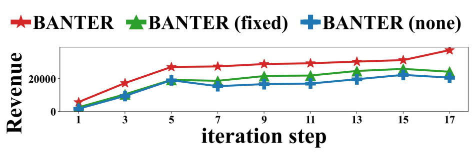

Fig. 12. Step-size scheduling comparison over initial steps.

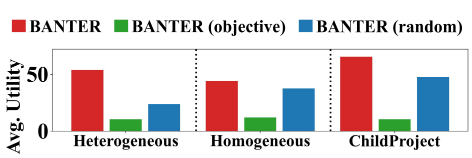

Fig. 13. Ablation tests replacing candidate sampling.

seller and customized NFT purchasing and breeding recommendations for individual buyers. By closely approximating competitive equilibrium, BANTER optimizes these outcomes for all stakeholders, including the seller and all buyers.

Revenue: BANTER outperforms all baselines by a significant margin, iteratively optimizing pricing through PRICEREC to assign higher prices to in-demand NFTs. LightGCN often secures the second-best performance by modeling buyer preferences, enabling more precise identification of optimal purchases and reducing item collisions. However, it fails to account for breeding and cannot provide dynamic pricing based on buyer demands. HetRecSys generates less revenue compared to BANTER and LightGCN, as its overemphasis on buyer-buyer and NFT-NFT relations can obscure the direct individual demand signals vital for effective dynamic pricing. NCF performs the worst because it fails to account for the alignment between buyer preferences and NFT attributes. Auction exhibits unstable performance, as its bidding process forces buyers to exhaust their budgets to secure top choices, leading to erratic results. Group struggles by recommending the same NFTs to groups of buyers, increasing the likelihood of popular NFTs being sold out and missing revenue opportunities. Lastly, Greedy performs variably, depending on the concentration of buyer preferences, as it greedily exploits the amalgamated valuation to provide recommendations.

Utility: For buyer utility, BANTER consistently delivers superior results. Most baselines only slightly improve their initial utilities. This stagnation indicates baselines' failure to identify NFT purchasing opportunities where the utility gained from NFTs (comprised of $U_{Instance}$, $U_{Collection}$, and $U_{Breeding}$ (Definition 5)) exceeds the cost of the NFTs. In contrast, BANTER excels by carefully estimating the NFT breeding utilities while calculating buyer-specific $U_{Collection}$ and objective $U_{Instance}$, allowing for effective evaluation of purchasing each NFT instance. Furthermore, while BANTER dynamically adjusts NFT prices based on demand, it also optimizes every buyer's purchasing based on the updated price and additional breeding utilities, resulting in the most advantageous options for buyers, leading to substantial improvement in buyer utilities.

When comparing different breeding mechanisms, BANTER generally achieves lower utility with Homogeneous Breeding than with Child-project Breeding due to the population factor f_{pop}, which reflects market saturation. Besides, BANTER attains higher utility with Heterogeneous Breeding for NFT projects with a larger number of NFT instances (*Axie Infinity* and *Bored Ape Yacht Club*) since it provides more options for buyers to choose the best parent sets. Additionally, BANTER demonstrates greater performance gains in *Axie Infinity*, which has a larger number of buyers and NFTs, necessitating equilibrium between pricing and purchasing recommendations. In contrast, BANTER's advantage over baselines is less significant in *CryptoKitties*, which has fewer buyers and a simpler market structure.

Runtime: BANTER achieves a balanced runtime, outperforming computationally expensive methods such as HetRecSys, NCF, and Auction, which require extensive training, inference, or prolonged bidding processes. While LightGCN occasionally demonstrates lower runtimes, it falls short of delivering high-quality recommendations for both buyers and sellers. Group benefits from lower runtimes due to its group-based recommendation strategy, and Greedy achieves the lowest runtimes because of its simplistic design, which comes at the expense of suboptimal results. When comparing breeding mechanisms, BANTER shows a slightly higher runtime in Homogeneous Breeding due to the additional computational cost for deriving the population factor f_{pop}. While Heterogeneous Breeding involves combinations of more than three parent NFTs, HPSS effectively accelerates the computation of the breeding utility, allowing BANTER to maintain a low runtime. Consistent with the derivation of Theorem 2, runtimes scale linearly with the size of the NFT project.

C. Scalability Tests

We conduct scalability tests on 1) a real-world Yelp review dataset with 16045 users and 38031 items [169] and 2) a large-scale synthetic dataset prepared by duplicating the number of buyers ranging from $10,000$ to $100,000$ for *Fat Ape Club*.[11]

First, we investigate the broader applicability of our proposed BANTER. This experiment aims to (1) assess BANTER's effectiveness in conventional scenarios and (2) explore the feasibility of treating real-world entities as NFTs. In particular, we adapt the Yelp dataset [169] for the NP^{3}R problem to simulate an NFT project within a conventional eCommerce context.[12]

Leveraging Yelp's extensive business attribute information, we filter "Restaurant" businesses and process their attributes. Based on the distribution of the data, we construct an NFT-like trait system, mimicking the attribute structure of NFT projects with five traits, including 1) "State," with attributes "PA," "FL," "TN," "MO," "IN," and "Other," 2) "Stars," with attributes "5.0," "4.5," "4.0," "3.5," "3.0," and "Other," 3) "Payment," with attributes "Both," "Bitcoin," "CreditCards," and "None," 4) "ToGo," with attributes "Both," "TakeOut," "Delivery," and "None," 5) "GoodFor" with attributes "Both," "Kids," "Meal," and "None." User reviews are analyzed to infer buyer preferences, while buyer budgets are assigned based on the number of reviews, which serves as a proxy of platform engagement; the supply count is set to 1 for all NFT instances. The final dataset comprises 16045 users as buyers and 38031 businesses as NFT instances. We employ the same baseline methods, breeding scenarios, and parameters for BANTER as the primary experiment above (Fig. 8).

Fig. 9 presents the comparison of seller's revenue, average buyers' utility, and runtime across different methods and breeding mechanisms applied to the Yelp dataset. As shown in Fig. 9, BANTER consistently outperforms all baselines in all cases, demonstrating its applicability to larger NFT projects with rich attributes. This superior performance is attributed to BANTER's comprehensive modeling of a multifaceted buyer utility (capturing instance, collection, and breeding values), whose alignment with individual optima is grounded in the duality properties of homogeneous functions, as established in Theorem 3.

Second, we evaluate the scalability of BANTER to a larger number of buyers. Fig. 10 presents a scalability test using synthetic data with the number of buyers N ranging from $10,000$ to $100,000$. Specifically, the number of NFT instances fixed at $M = 5,000$, the preferences and budget of buyers are randomly set and the breeding mechanism is set to Child-project Breeding. As shown in Fig. 10, BANTER consistently outperforms all baseline methods in terms of the seller's revenue while maintaining a low runtime in all large-scale settings, linearly increasing with the number of buyers.

D. Ablation Tests

We conduct ablation tests on *Fat Ape Club* to reveal the importance of different designs in BANTER. First, we contrast the equilibrium process in BANTER against the preference-aware pricing initialization INIT (see Algorithm 1). Fig. 11 compares BANTER under Homogeneous Breeding with two ablation variants after running for a fixed number of initial iteration steps: i) $\text{BANTER}_{\text{no init}}$, which eliminates the INIT initialization, and ii) INIT, which directly uses the pricing obtained by INIT without jointly refining the pricing and purchasing recommendation towards equilibrium. Comparing BANTER with $\text{BANTER}_{\text{no init}}$, the results show that while INIT helps BANTER by accelerating the optimization process, the equilibrium process contributes more significantly to BANTER's success in attaining optimal results (Proposition 1).

Second, we investigate the effectiveness of *demand-aware scheduling* for the pricing recommendation by comparing the attained revenue after running for a fixed number of initial iteration steps under Homogeneous Breeding. Fig. 12 compares BANTER with: i) $\text{BANTER}_{\text{fixed}}$, which adopts a fixed decay rate for the step size, and ii) $\text{BANTER}_{\text{none}}$, which does not adjust initial step size. The results demonstrate that the demand-aware scheduling in PRICE-REC assists BANTER in achieving the highest revenue, as it effectively adjusts the step sizes based on excess demand to accelerate convergence.

[11] Note that Auction is unsuitable for large-scale settings due to its combinatorial process of bidding across all buyers and all NFTs [168].

[12] We select the Yelp dataset [169] due to its size as well as rich business information and user reviews, which allow for a compelling simulation of NFT attributes and buyer preferences.

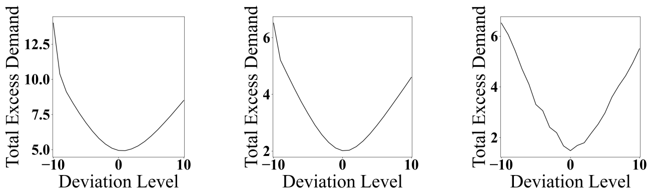

(a) BAYC (b) Fat Ape Club (c) Roaring Leader

Fig. 14. Comparing total excess demand ($\|\mathbf{z}\|_2$) to the deviation level from the optimal pricing given by BANTER.

Note that similar trends are also observed under Child-project Breeding and Heterogeneous Breeding.

Besides, we evaluate the impact of candidate selection $\mathcal{L}$ obtained by OPPS and HPSS in NFT-REC for the purchasing recommendation under all three breeding mechanisms. Fig. 13 compares BANTER with two variants: i) $\text{BANTER}_{\text{objective}}$, which selects the NFT η with the highest $V(\eta)$, and ii) $\text{BANTER}_{\text{random}}$, which selects random candidates. As shown, personalization achieved by the amalgamated valuation $\tilde{V}$ significantly outperforms other approaches in terms of average buyer utility across all breedings, while the contrast between BANTER and $\text{BANTER}_{\text{random}}$ clearly indicates the efficacy of both OPPS and HPSS.

E. Qualitative Tests

We analyze whether BANTER attains the market-clearing condition required by the competitive equilibrium. In particular, the pricing recommended by BANTER is uniformly adjusted by a certain percentage (termed the Deviation Level) up to $\pm 10\%$, and the total excess demand, which corresponds to the degree of difference between supply and demand, is subsequently measured under the new price using the buyer purchasing recommendations obtained through solving NFT-REC in the new price to estimate aggregate demand. The latter is quantified as the ℓ_2 norm of the excess demand vector $\|\mathbf{z}\|_2$. Fig. 14 compares the total excess demand under varied Deviation Levels (from -10% to $+10\%$). As shown in Fig. 14 for *Bored Ape Yacht Club (BAYC)*, *Fat Ape Club*, and *Roaring Leader*, respectively, the total excess demand reaches its minimum when the deviation level is precisely 0. This minimum point of excess demand signifies the closest approximation to market-clearing conditions, where supply and demand are most balanced. The outcome strongly supports the capability of BANTER to accurately achieve the equilibrium for NP^3R, effectively maximize seller revenue, and recommend appropriate NFTs to buyers for breeding.

VII. Conclusion

To the best of our knowledge, this paper is the first to study the NFT Project Pricing/Purchasing Recommendation (NP^3R) problem, which is challenging due to the *trait system* and the *breeding mechanisms*, including Heterogeneous, Homogeneous, and Child-project Breeding. We prove the hardness of NP^3R and design BANTER, a Breeding-aware NFT Equilibrium Recommendation method to tackle NP^3R, where PRICE-REC and NFT-REC iteratively update their recommendations for pricing and purchasing, respectively. Furthermore, OPPS and HPSS accelerate NFT-REC by effectively trimming the candidate parent sets for breeding utility calculation. Theoretical analyses prove the hardness of NP^3R and the convergence of BANTER to a competitive equilibrium, while experiments on five real-world NFT project data demonstrate the effectiveness of BANTER in generating more revenue for the seller and higher average utility for the buyers while maintaining high efficiency (with a low runtime) compared to the baseline methods. In our future work, we plan to study the impact of time and social influences on the price fluctuations of NFTs.

References

[1] Beeple. (2021) Everydays: The first 5000 days. [Online]. Available: https://onlineonly.christies.com/s/beeple-first-5000-days/beeple-b-1981-1/112924

[2] D. Labs. (2020) Nba top shot. [Online]. Available: https://nbatopshot.com/

[3] A. Perez. (2022) Nba top shot reaches $1b in sales amid nft market downturn. [Online]. Available: https://frontofficesports.com/nba-top-shot-reaches-1b-in-sales-amid-nft-market-downturn/

[4] D. Labs. (2022) Nfl all day. [Online]. Available: https://nflallday.com/

[5] ——. (2022) Ufc strike. [Online]. Available: https://ufcstrike.com/

[6] NHL. (2023) Nhl breakaway. [Online]. Available: https://nhlbreakaway.com/

[7] Nike. (2021) Nike acquires rtfkt. December 13, 2021. [Online]. Available: https://about.nike.com/en/newsroom/releases/nike-acquires-rtfkt

[8] A. Cheung. (2022) The dunk-inspired rtfkt x nike cryptokicks nft has been unveiled. Project websites: https://af1-lookbook.rtfkt.com/, https://rtfkt.com/faq/dunk-genesis. [Online]. Available: https://thesolesupplier.co.uk/news/the-dunk-inspired-rtfkt-x-nike-cryptokicks-nft-has-been-unveiled/

[9] J. Kastrenakes. (2021) Adidas is launching an nft collection with exclusive access to streetwear drops. Dec 16, 2021. [Online]. Available: https://www.theverge.com/2021/12/16/22822143/adidas-nft-launch-into-the-metaverse-price-release-date

[10] Adidas. (2021) Alts by adidas. Adidas. [Online]. Available: https://collect.adidas.com/

[11] S. S. . News. (2022) The starbucks odyssey begins. [Online]. Available: https://stories.starbucks.com/stories/2022/the-starbucks-odyssey-begins/

[12] H. C. (2023) Disney partners with dapper labs to launch nft platform featuring iconic disney characters. [Online]. Available: https://finance.yahoo.com/news/disney-partners-dapper-labs-launch-053227178.html

[13] D. Finzer and A. Atallah. (2017) Opensea. [Online]. Available: https://opensea.io/

[14] Binance. (2021) Binance nft. [Online]. Available: https://www.binance.com/en/nft/home

[15] B. Notheisen, J. B. Cholewa, and A. P. Shanmugam, “Trading real-world assets on blockchain: an application of trust-free transaction systems in the market for lemons,” *Business & Information Systems Engineering*, vol. 59, pp. 425–440, 2017.

[16] J. Kreppmeier, R. Laschinger, B. I. Steininger, and G. Dorfleitner, “Real estate security token offerings and the secondary market: Driven by crypto hype or fundamentals?” *Journal of Banking & Finance*, vol. 154, p. 106940, 2023.

[17] X. Liu, “Modeling users’ dynamic preference for personalized recommendation,” in *Twenty-fourth international joint conference on artificial intelligence*. International Joint Conferences on Artificial Intelligence Organization, 2015.

[18] H. Yang, T. Wang, X. Tang, Q. Li, Y. Shi, S. Jiang, H. Yu, and H. Song, “Multi-task learning for bias-free joint ctr prediction and market price modeling in online advertising,” in *Proceedings of the 30th ACM International Conference on Information & Knowledge Management*. New York, NY, USA: ACM, 2021, pp. 2291–2300.

[19] R. Kräussl and A. Tugnetti, "Non-fungible tokens (nfts): A review of pricing determinants, applications and opportunities," *Journal of Economic Surveys*, vol. 38, no. 2, pp. 555–574, 2024.

[20] D. Das, P. Bose, N. Ruaro, C. Kruegel, and G. Vigna, "Understanding security issues in the nft ecosystem," in *Proceedings of the 2022 ACM SIGSAC Conference on Computer and Communications Security*, 2022, pp. 667–681.

[21] T.-T. Pham and T.-D. Trinh, "Scoring model for nft evaluation," in *Proceedings of the 12th International Symposium on Information and Communication Technology*, 2023, pp. 157–164.

[22] A. Mekacher, A. Bracci, M. Nadini, M. Martino, L. Alessandretti, L. M. Aiello, and A. Baronchelli, "Heterogeneous rarity patterns drive price dynamics in nft collections," *Scientific reports*, vol. 12, no. 1, p. 13890, 2022.

[23] D. B. Naik, S. Terence, and A. Lydia, "Analysing non fungible tokens (nfts) and their rarity," in *2024 10th International Conference on Communication and Signal Processing (ICCSP)*. IEEE, 2024, pp. 1011–1015.

[24] C.-H. Wu, C.-Y. Liu, and T.-S. Weng, "Critical factors and trends in nft technology innovations," *Sustainability*, vol. 15, no. 9, p. 7573, 2023.

[25] M. Sawhney and P. Goodman, *Nike: Tiptoeing Into the Metaverse*. Kellogg School of Management, 2023.

[26] D. Vendrell. (2022) Rtfkt enters the real world. December 7, 2022. [Online]. Available: https://futureparty.com/rtfkt-physical-cryptokicks-irl-sneaker/

[27] X. He, K. Deng, X. Wang, Y. Li, Y. Zhang, and M. Wang, "Lightgcn: Simplifying and powering graph convolution network for recommendation," in *Proceedings of the 43rd International ACM SIGIR conference on research and development in Information Retrieval*, 2020, pp. 639–648.

[28] L. Yang, Z. Liu, Y. Dou, J. Ma, and P. S. Yu, "Consisrec: Enhancing gnn for social recommendation via consistent neighbor aggregation," in *Proceedings of the 44th international ACM SIGIR conference on Research and development in information retrieval*, 2021, pp. 2141–2145.

[29] J. Chang, C. Gao, X. He, D. Jin, and Y. Li, "Bundle recommendation with graph convolutional networks," in *Proceedings of the 43rd international ACM SIGIR conference on Research and development in Information Retrieval*, 2020, pp. 1673–1676.

[30] D. Cao, X. He, L. Miao, Y. An, C. Yang, and R. Hong, "Attentive group recommendation," in *The 41st International ACM SIGIR conference on research & development in information retrieval*. New York, NY, USA: ACM, 2018, pp. 645–654.

[31] Y. Labs. (2021) Bored ape yacht club # 4378. [Online]. Available: https://opensea.io/assets/ethereum/0xbc4ca0eda7647a8ab7c2061c2e118a18a936f13d/4378

[32] M. Collishaw. (2023) Heterosis. [Online]. Available: https://og.art/collections/heterosis/

[33] T. F. A. Club. (2021) Fat ape club. [Online]. Available: https://fatapeclub.io/

[34] Susha, G. N. B, and V. Vijay. (2021) Pann. [Online]. Available: https://opensea.io/assets/ethereum/0xb6dae651468e9593e4581705a09c10a76ac1e0c8/4284

[35] J.-S. Pang and M. Fukushima, "Quasi-variational inequalities, generalized nash equilibria, and multi-leader-follower games," *Computational Management Science*, vol. 2, no. 1, pp. 21–56, 2005.

[36] Y. K. Cheung, R. Cole, and N. Devanur, "Tatonnement beyond gross substitutes? gradient descent to the rescue," in *Proceedings of the forty-fifth annual ACM symposium on Theory of computing*. New York, NY, USA: ACM, 2013, pp. 191–200.

[37] W. Nicholson and C. M. Snyder, *Microeconomic theory: Basic principles and extensions*. Cengage Learning, 2012.

[38] S. Mavis. (2018) Axie infinity. [Online]. Available: https://axieinfinity.com/

[39] C. Banter. (2022) The problem with breeding games and how they can be solved. June 16, 2022 in Crypto News. [Online]. Available: https://www.cryptobanter.com/crypto-news/the-problem-with-breeding-games-and-how-they-can-be-solved/

[40] C. Dattoli. (2021) Roaring leader. [Online]. Available: http://side.xyz/roaring-leaders

[41] CryptoKitties. (2017) Mutations. CryptoKitties Guide. [Online]. Available: https://guide.cryptokitties.co/guide/cat-features/mutations

[42] F. Bears. (2023) Trait swap is a dynamic, composable nfts infrastructure & digital goods marketplace. [Online]. Available: https://www.traitswap.com/

[43] C. DiGiTAL. (2020, february) First supper - async art launch. [Online]. Available: https://danky.art/blog/first-supper-async-art

[44] J. Zhang, C. Gao, D. Jin, and Y. Li, "Group-buying recommendation for social e-commerce," in *2021 IEEE 37th International Conference on Data Engineering (ICDE)*. IEEE, 2021, pp. 1536–1547.

[45] R. Mugge and J. P. Schoormans, "Product design and apparent usability. the influence of novelty in product appearance," *Applied ergonomics*, vol. 43, no. 6, pp. 1081–1088, 2012.

[46] R. Lefkoff-Hagius and C. H. Mason, "Characteristic, beneficial, and image attributes in consumer judgments of similarity and preference," *Journal of Consumer Research*, vol. 20, no. 1, pp. 100–110, 1993.

[47] M. Fang, X. Zhou, Z. Zhang, C. Jin, and A. Zhou, "Seframe: an sgx-enhanced smart contract execution framework for permissioned blockchain," in *2022 IEEE 38th International Conference on Data Engineering (ICDE)*. IEEE, 2022, pp. 3166–3169.

[48] M. Fang, Z. Zhang, C. Jin, and A. Zhou, "High-performance smart contracts concurrent execution for permissioned blockchain using sgx," in *2021 IEEE 37th International Conference on Data Engineering (ICDE)*. IEEE, 2021, pp. 1907–1912.

[49] C. Zhang, C. Xu, H. Wang, J. Xu, and B. Choi, "Authenticated keyword search in scalable hybrid-storage blockchains," in *2021 IEEE 37th International Conference on Data Engineering (ICDE)*. IEEE, 2021, pp. 996–1007.

[50] H. Wang, C. Xu, C. Zhang, J. Xu, Z. Peng, and J. Pei, "vchain+: Optimizing verifiable blockchain boolean range queries," in *2022 IEEE 38th International Conference on Data Engineering (ICDE)*. IEEE, 2022, pp. 1927–1940.

[51] H. Bao and D. Roubaud, "Non-fungible token: A systematic review and research agenda," *Journal of Risk and financial management*, vol. 15, no. 5, p. 215, 2022.

[52] K. Vasan, M. Janosov, and A.-L. Barabási, "Quantifying nft-driven networks in crypto art," *Scientific reports*, vol. 12, no. 1, p. 2769, 2022.

[53] M. Nadini, L. Alessandretti, F. Di Giacinto, M. Martino, L. M. Aiello, and A. Baronchelli, "Mapping the nft revolution: market trends, trade networks, and visual features," *Scientific reports*, vol. 11, no. 1, p. 20902, 2021.

[54] Q. Wang, R. Li, Q. Wang, and S. Chen, "Non-fungible token (nft): Overview, evaluation, opportunities and challenges," *arXiv preprint arXiv:2105.07447*, 2021.

[55] H. Bao and D. Roubaud, "Recent development in fintech: Non-fungible token," pp. 44–46, 2021.

[56] T. Renduchintala, H. Alfauri, Z. Yang, R. D. Pietro, and R. Jain, "A survey of blockchain applications in the fintech sector," *Journal of Open Innovation: Technology, Market, and Complexity*, vol. 8, no. 4, p. 185, 2022.

[57] M. Foglia, G. Maci, and V. Pacelli, "Fintech and fan tokens: Understanding the risks spillover of digital asset investment," *Research in International Business and Finance*, vol. 68, p. 102190, 2024.

[58] R. Chohan and J. Paschen, "Nft marketing: How marketers can use nonfungible tokens in their campaigns," *Business Horizons*, vol. 66, no. 1, pp. 43–50, 2023.

[59] E. Sung, O. Kwon, and K. Sohn, "Nft luxury brand marketing in the metaverse: Leveraging blockchain-certified nfts to drive consumer behavior," *Psychology & Marketing*, 2023.

[60] R. Alkhudary, B. Belvaux, and N. Guibert, "Understanding non-fungible tokens (nfts): insights on consumption practices and a research agenda," *Marketing Letters*, vol. 34, no. 2, pp. 321–336, 2023.

[61] C. G. Senkardes, "Blockchain technology and nft s: a review in music industry," *Journal of Management, Marketing and Logistics-JMML*, vol. 8, no. 3, pp. 154–163, 2021.

[62] A.-D. Popescu, "Non-fungible tokens (nft)–innovation beyond the craze," in *5th International Conference on Innovation in Business, Economics and Marketing Research*, vol. 32, 2021, pp. 26–30.

[63] E. M. Kuehn, "A new business model in the fine arts realm based on nft certificates and pearl codes," *Digital Business*, p. 100079, 2024.

[64] B. Baker, A. Pizzo, Y. Su *et al.*, "Non-fungible tokens: a research primer and implications for sport management," *Faculty/Researcher Works*, 2022.

[65] E. Glebova and P. Mihail'Ova, "New currencies and new values in professional sports: blockchain, nft, and fintech through the stakeholder

approach," *Journal of Physical Education and Sport*, vol. 23, no. 5, 2023.

[66] D. Vidal-Tomás, "The new crypto niche: Nfts, play-to-earn, and metaverse tokens," *Finance research letters*, vol. 47, p. 102742, 2022.

[67] M. Dowling, "Is non-fungible token pricing driven by cryptocurrencies?" *Finance Research Letters*, vol. 44, p. 102097, 2022.

[68] ——, "Fertile land: Pricing non-fungible tokens," *Finance Research Letters*, vol. 44, p. 102096, 2022.

[69] Y. Wang, "Volatility spillovers across nfts news attention and financial markets," *International review of financial analysis*, vol. 83, p. 102313, 2022.

[70] H. Ko, B. Son, Y. Lee, H. Jang, and J. Lee, "The economic value of nft: Evidence from a portfolio analysis using mean–variance framework," *Finance Research Letters*, vol. 47, p. 102784, 2022.

[71] I. Ghosh, E. Alfaro-Cortés, M. Gámez, and N. García-Rubio, "Prediction and interpretation of daily nft and defi prices dynamics: Inspection through ensemble machine learning & xai," *International Review of Financial Analysis*, vol. 87, p. 102558, 2023.

[72] S. Gunay, J. W. Goodell, S. Muhammed, and D. Kirimhan, "Frequency connectedness between fintech, nft and defi: Considering linkages to investor sentiment," *International Review of Financial Analysis*, vol. 90, p. 102925, 2023.

[73] S. Bhujel and Y. Rahulamathavan, "A survey: Security, transparency, and scalability issues of nft's and its marketplaces," *Sensors*, vol. 22, no. 22, p. 8833, 2022.

[74] V. von Wachter, J. R. Jensen, F. Regner, and O. Ross, "Nft wash trading: Quantifying suspicious behaviour in nft markets," in *International Conference on Financial Cryptography and Data Security*. Springer, 2022, pp. 299–311.

[75] Z. Wang, J. Gao, and X. Wei, "Do nfts' owners really possess their assets? a first look at the nft-to-asset connection fragility," in *Proceedings of the ACM Web Conference 2023*, 2023, pp. 2099–2109.

[76] R. A. A. Mochram, C. T. Makawowor, K. M. Tanujaya, J. V. Moniaga, and B. A. Jabar, "Systematic literature review: blockchain security in nft ownership," in *2022 International Conference on Electrical and Information Technology (IEIT)*. IEEE, 2022, pp. 302–306.

[77] F. Stöger, A. Zhou, H. Duan, and A. Perrig, "Demystifying web3 centralization: The case of off-chain nft hijacking," in *International Conference on Financial Cryptography and Data Security*. Springer, 2023, pp. 182–199.

[78] Y. Gao, M. Saad, A. Oest, J. Zhang, B. Han, and S. Chen, "Can i own your nfts? understanding the new attack surface to nfts," *IEEE Communications Magazine*, vol. 61, no. 9, pp. 64–70, 2023.

[79] D. Costa, L. La Cava, and A. Tagarelli, "Show me your nft and i tell you how it will perform: Multimodal representation learning for nft selling price prediction," in *Proceedings of the ACM Web Conference 2023*, 2023, pp. 1875–1885.

[80] A. Kapoor, D. Guhathakurta, M. Mathur, R. Yadav, M. Gupta, and P. Kumaraguru, "Tweetboost: Influence of social media on nft valuation," in *Companion Proceedings of the Web Conference 2022*, 2022, pp. 621–629.

[81] S. Casale-Brunet, M. Zichichi, L. Hutchinson, M. Mattavelli, and S. Ferretti, "The impact of nft profile pictures within social network communities," in *Proceedings of the 2022 ACM Conference on Information Technology for Social Good*. New York, NY, USA: ACM, 2022, pp. 283–291.

[82] R. Sawhney, M. Thakkar, R. Soun, A. Neerkaje, V. Sharma, D. Guhathakurta, and S. Chava, "Tweet based reach aware temporal attention network for nft valuation," in *Findings of the Association for Computational Linguistics: EMNLP 2022*, 2022, pp. 6321–6332.

[83] D. Piyadigama and G. Poravi, "An analysis of the features considerable for nft recommendations," in *2022 15th International Conference on Human System Interaction (HSI)*. IEEE, 2022, pp. 1–7.

[84] N. Edi Surya, S. Sulaiman, M. Ria Andryani, M. Kom, M. Ria Andryani, M. Kom, S. Prihambodo Hendro, and W. Yeni, "Recommendation system with content-based filtering in nft marketplace," *Journal of Advances in Information Technology*, vol. 14, no. 3, pp. 518–522, 2023.

[85] D. Aydoğdu and N. Aydın, "Recommender systems for nft purchasing," in *2023 4th International Informatics and Software Engineering Conference (IISEC)*. IEEE, 2023, pp. 1–5.

[86] S. Kim, Y. Lee, Y. Kim, J. Hong, and Y. Lee, "Nfts to mars: Multi-attention recommender system for nfts," *arXiv preprint arXiv:2306.10053*, 2023.

[87] M. Choi, S. Kim, Y. Kim, Y. Lee, J. Hong, and Y. Lee, "A recommender system for nft collectibles with item feature," *arXiv preprint arXiv:2403.18305*, 2024.

[88] K. Ren, J. Qin, L. Zheng, Z. Yang, W. Zhang, and Y. Yu, "Deep landscape forecasting for real-time bidding advertising," in *Proceedings of the 25th ACM SIGKDD international conference on knowledge discovery & data mining*. New York, NY, USA: ACM, 2019, pp. 363–372.

[89] L. Zheng, P. Cheng, and L. Chen, "Auction-based order dispatch and pricing in ridesharing," in *2019 IEEE 35th International Conference on Data Engineering (ICDE)*, IEEE. Washington, DC, USA: IEEE Computer Society, 2019, pp. 1034–1045.

[90] W. Zhang, H. Liu, J. Han, Y. Ge, and H. Xiong, "Multi-agent graph convolutional reinforcement learning for dynamic electric vehicle charging pricing," in *Proceedings of the 28th ACM SIGKDD conference on knowledge discovery and data mining*. New York, NY, USA: ACM, 2022, pp. 2471–2481.

[91] Y. Tong, D. Shi, Y. Xu, W. Lv, Z. Qin, and X. Tang, "Combinatorial optimization meets reinforcement learning: Effective taxi order dispatching at large-scale," *IEEE Transactions on Knowledge and Data Engineering*, 2021.

[92] F. Zhu, W. Xiao, Y. Yu, Z. Wang, Z. Chen, Q. Lu, Z. Liu, M. Wu, and S. Ni, "Modeling price elasticity for occupancy prediction in hotel dynamic pricing," in *Proceedings of the 31st ACM International Conference on Information & Knowledge Management*. New York, NY, USA: ACM, 2022, pp. 4742–4746.

[93] H. Zhu, E. Chen, H. Xiong, K. Yu, H. Cao, and J. Tian, "Mining mobile user preferences for personalized context-aware recommendation," *ACM Transactions on Intelligent Systems and Technology (TIST)*, vol. 5, no. 4, pp. 1–27, 2014.

[94] Q. Liu, S. Wu, and L. Wang, "Deepstyle: Learning user preferences for visual recommendation," in *Proceedings of the 40th international acm sigir conference on research and development in information retrieval*. New York, NY, USA: ACM, 2017, pp. 841–844.

[95] X. Chen, H. Chen, H. Xu, Y. Zhang, Y. Cao, Z. Qin, and H. Zha, "Personalized fashion recommendation with visual explanations based on multimodal attention network: Towards visually explainable recommendation," in *Proceedings of the 42nd International ACM SIGIR Conference on Research and Development in Information Retrieval*, 2019, pp. 765–774.

[96] S. Zhang, L. Yao, A. Sun, and Y. Tay, "Deep learning based recommender system: A survey and new perspectives," *ACM computing surveys (CSUR)*, vol. 52, no. 1, pp. 1–38, 2019.

[97] Y. Koren, R. Bell, and C. Volinsky, "Matrix factorization techniques for recommender systems," *Computer*, vol. 42, no. 8, pp. 30–37, 2009.

[98] X. Zhou, L. Chen, Y. Zhang, D. Qin, L. Cao, G. Huang, and C. Wang, "Enhancing online video recommendation using social user interactions," *The VLDB Journal*, vol. 26, pp. 637–656, 2017.

[99] X. Zhou, D. Qin, L. Chen, and Y. Zhang, "Real-time context-aware social media recommendation," *The VLDB Journal*, vol. 28, pp. 197–219, 2019.

[100] T. Zhu, P. Harrington, J. Li, and L. Tang, "Bundle recommendation in ecommerce," in *Proceedings of the 37th international ACM SIGIR conference on Research & development in information retrieval*, 2014, pp. 657–666.

[101] L. A. M. C. Carvalho and H. T. Macedo, "Users' satisfaction in recommendation systems for groups: an approach based on noncooperative games," in *Proceedings of the 22nd international conference on world wide web*. New York, NY, USA: International World Wide Web Conferences Steering Committee / ACM, 2013, pp. 951–958.

[102] H. Zhao, Q. Liu, Y. Ge, R. Kong, and E. Chen, "Group preference aggregation: A nash equilibrium approach," in *2016 IEEE 16th International Conference on Data Mining (ICDM)*. IEEE, 2016, pp. 679–688.

[103] L. Zhang, R. Zhou, H. Jiang, H. Wang, and Y. Zhang, "Item group recommendation: a method based on game theory," in *Proceedings of the 26th international conference on world wide web companion*, 2017, pp. 1405–1411.

[104] L. Xiao, Z. Min, Z. Yongfeng, G. Zhaoquan, L. Yiqun, and M. Shaoping, "Fairness-aware group recommendation with pareto-efficiency," in *Proceedings of the eleventh ACM conference on recommender systems*, 2017, pp. 107–115.

[105] W. Wu, M.-Y. Yeh, and M.-S. Chen, "Deep censored learning of the winning price in the real time bidding," in *Proceedings of the 24th*

ACM SIGKDD International Conference on Knowledge Discovery & Data Mining. New York, NY, USA: ACM, 2018, pp. 2526–2535.
[106] Y. Ge, S. Liu, R. Gao, Y. Xian, Y. Li, X. Zhao, C. Pei, F. Sun, J. Ge, W. Ou *et al.*, "Towards long-term fairness in recommendation," in *Proceedings of the 14th ACM international conference on web search and data mining*, 2021, pp. 445–453.
[107] A. Singh and T. Joachims, "Fairness of exposure in rankings," in *Proceedings of the 24th ACM SIGKDD international conference on knowledge discovery & data mining*, 2018, pp. 2219–2228.
[108] R. Burke, N. Sonboli, and A. Ordonez-Gauger, "Balanced neighborhoods for multi-sided fairness in recommendation," in *Conference on fairness, accountability and transparency*. PMLR, 2018, pp. 202–214.
[109] T. Sühr, A. J. Biega, M. Zehlike, K. P. Gummadi, and A. Chakraborty, "Two-sided fairness for repeated matchings in two-sided markets: A case study of a ride-hailing platform," in *Proceedings of the 25th ACM SIGKDD International Conference on Knowledge Discovery & Data Mining*, 2019, pp. 3082–3092.
[110] Y. Ge, X. Zhao, L. Yu, S. Paul, D. Hu, C.-C. Hsieh, and Y. Zhang, "Toward pareto efficient fairness-utility trade-off in recommendation through reinforcement learning," in *Proceedings of the fifteenth ACM international conference on web search and data mining*, 2022, pp. 316–324.
[111] X. Lin, H. Chen, C. Pei, F. Sun, X. Xiao, H. Sun, Y. Zhang, W. Ou, and P. Jiang, "A pareto-efficient algorithm for multiple objective optimization in e-commerce recommendation," in *Proceedings of the 13th ACM Conference on recommender systems*, 2019, pp. 20–28.
[112] Y. Zheng, C. Gao, X. He, Y. Li, and D. Jin, "Price-aware recommendation with graph convolutional networks," in *2020 IEEE 36th International Conference on Data Engineering (ICDE)*, IEEE. Washington, DC, USA: IEEE Computer Society, 2020, pp. 133–144.
[113] C. Pei, X. Yang, Q. Cui, X. Lin, F. Sun, P. Jiang, W. Ou, and Y. Zhang, "Value-aware recommendation based on reinforcement profit maximization," in *The World Wide Web Conference*, 2019, pp. 3123–3129.
[114] X. Zhang, B. Xu, L. Yang, C. Li, F. Ma, H. Liu, and H. Lin, "Price does matter! modeling price and interest preferences in session-based recommendation," in *Proceedings of the 45th International ACM SIGIR Conference on Research and Development in Information Retrieval*, 2022, pp. 1684–1693.
[115] P. Xia, B. Liu, Y. Sun, and C. Chen, "Reciprocal recommendation system for online dating," in *Proceedings of the 2015 IEEE/ACM International Conference on Advances in Social Networks Analysis and Mining 2015*, 2015, pp. 234–241.
[116] N. Freeman. (2023) Sbf, bored ape yacht club, and the spectacular hangover after the art world's nft gold rush. January 18, 2023. [Online]. Available: https://www.vanityfair.com/style/2023/01/sbf-bored-apes-art-world-hangover
[117] C. Daskalakis, P. W. Goldberg, and C. H. Papadimitriou, "The complexity of computing a nash equilibrium," *Communications of the ACM*, vol. 52, no. 2, pp. 89–97, 2009.
[118] N. R. Devanur, C. H. Papadimitriou, A. Saberi, and V. V. Vazirani, "Market equilibrium via a primal–dual algorithm for a convex program," *Journal of the ACM (JACM)*, vol. 55, no. 5, pp. 1–18, 2008.
[119] X. Li, Q. Luo, X. Fu, and S. Cai, "What motivates people to purchase nfts? a self-discrepancy perspective," in *PACIS 2023 Proceedings*, 2023, p. 94. [Online]. Available: https://aisel.aisnet.org/pacis2023/94
[120] E. J. North, R. B. De Vos, and T. Kotze, "The importance of apparel product attributes for female buyers," *Journal of Consumer Sciences*, vol. 31, 2003.
[121] Y.-K. Che and I. Gale, "The optimal mechanism for selling to a budget-constrained buyer," *Journal of Economic theory*, vol. 92, no. 2, pp. 198–233, 2000.
[122] K.-H. Ho, Y. Hou, T.-T. Chan, and H. Pan, "Analysis of non-fungible token pricing factors with machine learning," in *2022 IEEE International Conference on Systems, Man, and Cybernetics (SMC)*. IEEE, 2022, pp. 1161–1166.
[123] A. Serada, T. Sihvonen, and J. T. Harviainen, "Cryptokitties and the new ludic economy: how blockchain introduces value, ownership, and scarcity in digital gaming," *Games and Culture*, vol. 16, no. 4, pp. 457–480, 2021.
[124] X. Wang, X. He, M. Wang, F. Feng, and T.-S. Chua, "Neural graph collaborative filtering," in *Proceedings of the 42nd international ACM SIGIR conference on Research and development in Information Retrieval*, 2019, pp. 165–174.
[125] R. Nourmohammadi, M. Arabian, M. Ghorbanpour, M. M. Nazemi, and N. Nezhadsistani, "Nft scoring: An analysis of the considerable features," in *Proceedings of the 2022 5th International Conference on Blockchain Technology and Applications*, 2022, pp. 57–62.
[126] W. Xiong, Y. Wang, W. Li, J. Zhang, and H. Guo, "Pricing mechanism of non-fungible token (nft) driven by rarity design," in *2023 IEEE International Conference on Blockchain (Blockchain)*. IEEE, 2023, pp. 74–79.
[127] R. Sniper. Bored ape yacht club traits. [Online]. Available: https://raritysniper.com/bored-ape-yacht-club/traits
[128] F. TOOLS. Axie trait stats. [Online]. Available: https://freakitties.github.io/axie/traitstats.html
[129] K. Helper. (2017) Cryptokitties traits rarity table by kitties count. [Online]. Available: https://kittyhelper.co/tools/traits-rarity/
[130] R. Hofstetter, M. P. Fritze, and C. Lamberton, "Beyond scarcity: A social value-based lens for nft pricing," *Journal of Consumer Research*, vol. 51, no. 1, pp. 140–150, 2024.
[131] S. Mereu, "Nft sports collectibles: Characteristics and factors of consumer value," in *Global Applications of the Internet of Things in Digital Marketing*. IGI Global, 2023, pp. 310–331.
[132] D. Wang, Q. Ren, X. Li, Y. Qi, and Q. Zhou, "Defining consumers' interest and future of nft fashion," in *2022 International Conference on Social Sciences and Humanities and Arts (SSHA 2022)*. Atlantis Press, 2022, pp. 584–594.
[133] B. C. Ooi, G. Chen, M. Z. Shou, K.-L. Tan, A. Tung, X. Xiao, J. W. L. Yip, B. Zhang, and M. Zhang, "The metaverse data deluge: What can we do about it?" in *2023 IEEE 39th International Conference on Data Engineering (ICDE)*. IEEE, 2023, pp. 3675–3687.
[134] Spatial. (2022, sep) What is an nft gallery? 5 galleries to visit in spatial! [Online]. Available: https://www.spatial.io/blog/what-is-an-nft-gallery-and-5-galleries-to-visit-in-spatial
[135] J. Pastor. (2023) What is cryptovoxels? March 29, 2023. [Online]. Available: https://www.stadioplus.com/post/what-is-cryptovoxels
[136] B. Nolan. Voxels. [Online]. Available: https://www.voxels.com/
[137] O. H. Center. (2023, june) How do i turn on collection offers for traits? [Online]. Available: https://support.opensea.io/hc/en-us/articles/7351055986323-How-do-I-turn-on-collection-offers-for-traits-
[138] D. Daye. (2022, july) The ultimate guide for nft traits. [Online]. Available: https://chainwitcher.com/the-ultimate-guide-for-nft-traits/
[139] OpenSea. How to make the most of your opensea collection. December 11, 2022. [Online]. Available: https://opensea.io/learn/nft/optimize-nft-collection-page
[140] R. Layard, G. Mayraz, and S. Nickell, "The marginal utility of income," *Journal of Public Economics*, vol. 92, no. 8-9, pp. 1846–1857, 2008.
[141] K. Hu, W. Hsu, and M. L. Lee, "Utilizing users' tipping points in e-commerce recommender systems," in *2013 IEEE 29th International Conference on Data Engineering (ICDE)*. IEEE, 2013, pp. 494–504.
[142] N. Hurley and M. Zhang, "Novelty and diversity in top-n recommendation–analysis and evaluation," *ACM Transactions on Internet Technology (TOIT)*, vol. 10, no. 4, pp. 1–30, 2011.
[143] N. K. Andy Chorlian. (2021) Fractional.art: Decentralized protocol for collective ownership of nfts. [Online]. Available: https://fractional.art/
[144] A. Takyar. (2021) Fractional nfts. [Online]. Available: https://www.leewayhertz.com/fractional-nft/
[145] R. Games. Rowa mechanics part 6: Nft minting & breeding. Published in Rowa Games, 2 min read, Mar 16, 2023. [Online]. Available: https://blog.rowa.games/rowa-mechanics-part-6-nft-minting-breeding-3c6743187e54
[146] PERPLAY. [ama july] part.4 — nft what is the probability of obtaining a special box when combining rare+rare? Published in PERPLAY, 3 min read, Jul 31, 2023. [Online]. Available: https://medium.com/@PERPLAY/ama-july-part-4-nft-615ad22a82d5
[147] K. Benouaret and K.-L. Tan, "Probabilistic majority rule-based group recommendation," in *2023 IEEE 39th International Conference on Data Engineering (ICDE)*. IEEE, 2023, pp. 1489–1501.
[148] N. Zhang, Y. Tian, and J. M. Patel, "Discovery-driven graph summarization," in *2010 IEEE 26th international conference on data engineering (ICDE 2010)*. IEEE, 2010, pp. 880–891.
[149] K. J. Arrow and G. Debreu, "Existence of an equilibrium for a competitive economy," *Econometrica: Journal of the Econometric Society*, pp. 265–290, 1954.
[150] R. C. Raimondo, "Market clearing, utility functions, and securities prices," *Economic Theory*, vol. 25, pp. 265–285, 2005.

[151] M. Khorasany, Y. Mishra, and G. Ledwich, “Market framework for local energy trading: A review of potential designs and market clearing approaches,” *IET Generation, Transmission & Distribution*, vol. 12, no. 22, pp. 5899–5908, 2018.

[152] E. Eisenberg, “Aggregation of utility functions,” *Management Science*, vol. 7, no. 4, pp. 337–350, 1961.

[153] ——, “Duality in homogeneous programming,” *Proceedings of the American Mathematical Society*, vol. 12, no. 5, pp. 783–787, 1961.

[154] Y. Nesterov *et al.*, *Lectures on convex optimization*. Springer, 2018, vol. 137.

[155] W. J. Reed, “The pareto, zipf and other power laws,” *Economics letters*, vol. 74, no. 1, pp. 15–19, 2001.

[156] Z. Zolaktaf, R. Babanezhad, and R. Pottinger, “A generic top-n recommendation framework for trading-off accuracy, novelty, and coverage,” in *2018 IEEE 34th International Conference on Data Engineering (ICDE)*. IEEE, 2018, pp. 149–160.

[157] F. M. Ivan Liljeqvist. (2022) Moralis web3 technology. [Online]. Available: https://moralis.io/

[158] Y. Labs. (2021) Bored ape yacht club. [Online]. Available: https://boredapeyachtclub.com/

[159] A. Zen. (2017) Crypto kitties. [Online]. Available: https://www.cryptokitties.co/

[160] T. F. A. Club. (2022) Fat ape babies club. [Online]. Available: https://opensea.io/collection/fat-ape-babies-club

[161] C.-Y. Yeh, H.-W. Chen, D.-N. Yang, W.-C. Lee, P. S. Yu, and M.-S. Chen, “Planning data poisoning attacks on heterogeneous recommender systems in a multiplayer setting,” in *2023 IEEE 39th International Conference on Data Engineering (ICDE)*, IEEE. Washington, DC, USA: IEEE Computer Society, 2023, pp. 2510–2523.

[162] K. Kang, J. Park, W. Kim, H. Choe, and J. Choo, “Recommender system using sequential and global preference via attention mechanism and topic modeling,” in *Proceedings of the 28th ACM international conference on information and knowledge management*. New York, NY, USA: ACM, 2019, pp. 1543–1552.

[163] S. Kang, W. Kweon, D. Lee, J. Lian, X. Xie, and H. Yu, “Unbiased, effective, and efficient distillation from heterogeneous models for recommender systems,” *ACM Transactions on Recommender Systems*, vol. 3, no. 3, pp. 1–28, 2025.

[164] G. Lee, K. Kim, and K. Shin, “Revisiting lightgcn: Unexpected inflexibility, inconsistency, and a remedy towards improved recommendation,” in *Proceedings of the 18th ACM Conference on Recommender Systems*, 2024, pp. 957–962.

[165] X. He, L. Liao, H. Zhang, L. Nie, X. Hu, and T.-S. Chua, “Neural collaborative filtering,” in *Proceedings of the 26th international conference on world wide web*, 2017, pp. 173–182.

[166] L. Guo, H. Yin, Q. Wang, B. Cui, Z. Huang, and L. Cui, “Group recommendation with latent voting mechanism,” in *2020 IEEE 36th International Conference on Data Engineering (ICDE)*, IEEE. Washington, DC, USA: IEEE Computer Society, 2020, pp. 121–132.

[167] C. Zhou, G. Zou, S. Hu, H. Lv, L. Wu, and B. Zhang, “Dual-graph convolutional network and dual-view fusion for group recommendation,” in *Pacific-Asia Conference on Knowledge Discovery and Data Mining*. Springer, 2024, pp. 231–243.

[168] R. Garg and S. Kapoor, “Auction algorithms for market equilibrium,” in *Proceedings of the thirty-sixth annual ACM symposium on Theory of computing*, 2004, pp. 511–518.

[169] Y. Inc., “Yelp review dataset,” 2015, accessed: 2024-08-05. [Online]. Available: https://www.yelp.com/dataset